BMC Plant Biology

RESEARCH

Open Access

Tissue-specific transcriptomic analysis reveals the molecular mechanisms responsive to cold stress in *Poa crymophila*, and development of EST-SSR markers linked to cold tolerance candidate genes

Liuban Tang[1], Yuying Zheng[1], Huanhuan Lu[1], Yongsen Qiu[1], Huizhi Wang[1], Haoqin Liao[1] and Wengang Xie[1*]

Abstract

Background *Poa crymophila* is a perennial, cold-tolerant, native grass species, widely distributed in the Qinghai-Tibet Plateau. However, the tissue-specific regulatory mechanisms and key regulatory genes underlying its cold tolerance remain poorly characterized. Therefore, in this study, based on the screening and evaluation of cold tolerance of four *Poa* species, the cold tolerance mechanism of *P. crymophila*'s roots, stems, and leaves and its cold tolerance candidate genes were investigated through physiological and transcriptomic analyses.

Results Results of the present study suggested that the cold tolerance of the four *Poa* species was in the following order: *P. crymophila* > *P. botryoides* > *P. pratensis* var. anceps > *P. pratensis*. Cold stress significantly changed the physiological characteristics of roots, stems, and leaves of *P. crymophila* in this study. In addition, the transcriptome results showed that 4434, 8793, and 14,942 differentially expressed genes (DEGs) were identified in roots, stems, and leaves, respectively; however, 464 DEGs were commonly identified in these three tissues. KEGG enrichment analysis showed that these DEGs were mainly enriched in the phenylpropanoid biosynthesis pathway (roots), photosynthesis pathway (stems and leaves), circadian rhythm-plant pathway (stems and leaves), starch and sucrose metabolism pathway (roots, stems, and leaves), and galactose metabolism pathway (roots, stems, and leaves). A total of 392 candidate genes involved in Ca^{2+} signaling, ROS scavenging system, hormones, circadian clock, photosynthesis, and transcription factors (TFs) were identified in *P. crymophila*. Weighted gene co-expression network analysis (WGCNA) identified nine hub genes that may be involved in *P. crymophila* cold response. A total of 200 candidate gene-based EST-SSRs were developed and characterized. Twenty-nine polymorphic EST-SSRs primers were finally used to study genetic diversity of 40 individuals from four *Poa* species with different cold tolerance characteristics. UPGMA cluster and STRUCTURE analysis showed that the 40 *Poa* individuals were clustered into three major groups, individual plant with similar cold tolerance tended to group together. Notably, markers P37 (*PcGA2ox3*) and P148 (*PcERF013*) could distinguish *P. crymophila* from *P. pratensis* var. anceps, *P. pratensis*, and *P. botryoides*.

*Correspondence:
Wengang Xie
xiewg@lzu.edu.cn

Full list of author information is available at the end of the article

Conclusions This study provides new insights into the molecular mechanisms underlying the cold tolerance of *P. crymophila*, and also lays a foundation for molecular marker-assisted selection for cold tolerance improvement in *Poa* species.

Keywords *Poa crymophila*, Cold stresses, Physiology, Transcriptome analysis, Weighted gene co-expression network analysis (WGCNA), Molecular marker-assisted selection (MAS), Genetic diversity

Background

Global climate change poses escalating threats to agricultural productivity, with cold stress emerging as a critical abiotic constraint on plant growth, developmental cycles, and biogeographical patterns [1, 2]. The economic repercussions are staggering-cold-induced crop losses exceed $2 billion annually, including devastating impacts on over 13 million hectares of rice cultivation [3, 4]. This underscores the urgent need to decipher plant cold adaptation mechanisms, where elucidating the molecular and physiological basis of cold tolerance could revolutionize breeding strategies to enhance crop resilience and safeguard global food security.

Plants have evolved multiple methods to respond to cold stress during long-term environmental adaptations [5]. Cold stress signals are first sensed by the outer parts of the plant through a highly organized signaling system that further generates a series of response mechanisms in vivo [6]. These responses mainly include modification of the membrane lipid composition, synthesis of osmoprotectants, activating the ROS (Reactive oxygen species) scavenging system, signaling cascade, and changes in the expression profile of cold-responsive genes [5, 7]. ICE (Inducer of CBF Expression) is a MYC-type bHLH transcription factor, including *ICE1* and *ICE2*, which induces and positively regulates the expression of the *CBFs*, which enhances cold tolerance in *Arabidopsis thaliana* [8, 9]. Additionally, *CBFs/DREBs*, which include *CBF1/DREB1B*, *CBF2/DREB1C*, and *CBF3/DREB1A*, are transcription factors (TFs) of the AP2/ERF family that regulate the expression of CORs (Cold-regulated genes) [10, 11]. These genes encode osmoprotectants, protein kinases, lipids, hormones, and proteins, and directly participate in responding to cold stress to enhance plant tolerance [2, 12]. Consequently, *ICE*, *CBFs*, and *CORs* constitute a crucial signaling pathway, the ICE-CBF-COR cascade which mitigates cold stress in plants [13].

In addition, plant responses to cold stress are regulated by other factors such as Ca^{2+} signaling, hormones, circadian rhythms, and photosynthesis [7, 12]. The Ca^{2+} signaling pathway is considered as most common cold response pathway in plants, including CaM (Calmodulin), CML (Calmodulin-like protein), CBL (Calcineurin B-like protein), CIPK (CBL interacting protein kinase), CPK/CDPK (Calcium-dependent protein kinase), CAMTA (Calmodulin-binding transcription activator), which interact and regulate the CBF/DREB1 genes in response to cold stress [5, 12]. Moreover, Ca^{2+} signaling coordinates with ROS and ABA to converge on the MAPK cascade via phosphorylation relays [2]. ROS induces the expression of TFs through the accumulation of plant hormones, and TFs alleviate the damage of ROS by regulating the expression of ROS responsive genes [2, 14]. Recent studies suggest that photosynthesis and circadian rhythms pathways are crucial pathways that play an important role in cold stress tolerance [15]. CBF genes are not only induced by cold stress but also regulated by the circadian clock and light signals [16].

Besides, in the recent years, transcriptome studies have provided a new perspective for researching the plant response to cold stress [3, 17]. A previous study reported that the plant circadian pathway was crucial for *Helictotrichon virescens*'s response to cold stress; the expression of DEGs encoding *LHY* and *HY5* was strongly up-regulated during cold stress [17]. Transcriptome analysis revealed that Ca^{2+}, ROS, hormone signaling, the circadian clock, and photosynthetic antenna proteins may significantly contribute to cold tolerance in *Vicia sativa* L. through CBF-dependent or independent transcriptional pathways [18]. Transcriptome analysis of *Triticum aestivum* L. at 4 °C low-temperature showed that starch and sucrose metabolism, glutathione metabolism, and plant hormone signal transduction pathways were significantly enriched, and many genes belonging to the bHLH, MYB, NAC, WRKY, and ERF TF families were highly expressed [19]. Additionally, the WGCNA identified several key genes involved in seedlings development under cold stress [19]. Thus, previous studies demonstrated that transcriptome analysis could unveil the molecular mechanisms behind plant stress tolerance and explore the potential functions of crucial genes. Moreover, SSR or EST-SSR molecular markers, developed based on candidate genes, are intimately associated with key agronomic traits. These markers serve as valuable tools to enhance genetic improvement and facilitate molecular marker-assisted selection in plants [20, 21].

The Qinghai-Tibet Plateau is known as the Roof of the World, the Third Pole and the Water Tower of Asia, which is an important shield for China's ecological security, as well as an important animal husbandry production base [22]. However, the Qinghai-Tibet Plateau has a typical plateau continental climate, with a large temperature difference between day and night, low annual average temperature, and a short frost-free period which

shows the average monthly temperature is between −20 °C and −10 °C [23, 24]. The extreme climatic conditions of the Qinghai-Tibet Plateau impose selective pressures on the evolution of phenotypic and physiological characteristics. Many native species including *Elymus nutans*, *E. sibicicus*, *P. pratensis* and *P. crymophila* are widely distributed and utilized species on the Qinghai-Tibet Plateau due to their strong environmental adaptability and long-term natural domestication [23, 25, 26]. Of these native grasses, *P. crymophila* is widely distributed in humid grasslands, alpine grasslands, forest margins, hillsides, valleys, and tidal flats at an altitude of 2150 ~ 4800 m on the Qinghai-Tibet Plateau [23]. After more than 30 years of selection, cultivation, and domestication, *P. crymophila* has been cultivated as an ecological grass variety widely used in ecological restoration of degraded grassland in the alpine region. It has excellent cold tolerance and can survive at about −40 °C [23]. However, the physiological and molecular mechanisms behind the cold stress tolerance and role of key regulatory genes and pathways of *P. crymophila* are poorly understood yet.

Therefore, this study focused on cold-adapted *P. crymophila* species from the Qinghai-Tibet Plateau, the tissue-specific response mechanism of cold tolerance was explored through physiological and transcriptomic analyses under 4 °C cold stress, and candidate genes for cold tolerance were identified. Additionally, molecular markers were developed based on these candidate cold-tolerant genes to conduct molecular genetic diversity analysis and cold tolerance screening of different *Poa* species. These findings initially revealed the unique efficient cold response and adaptive regulatory capabilities of *P. crymophila*, offering new perspectives on the early regulatory physiological and molecular mechanisms of its cold tolerance. This research also lays a foundation for molecular marker-assisted selection for cold tolerance improvement in *Poa* species.

Materials and methods

Plant growing conditions and sample collection

Seeds of *P. crymophila* Keng cv. Qinghai, *P. pratensis* L. var. anceps Gaud. cv. Qinghai, *P. pratensis* L. cv. Qinghai, and *P. botryoides* were obtained from the Qinghai Academy of Animal Husbandry and Veterinary Science. Following 4 °C vernalization (3 d), seeds were sown in 0.5-L pots (5 plants/pot) containing standardized substrate (black soil: peat = 2:1, v/v). Seedlings were cultivated under controlled conditions: 25/20°C day/night cycle, 16 h light/8 h dark photoperiod, 500 μmol m^{-2} s^{-1} light intensity, and 70% relative humidity.

There were 10 pots of each species, totaling 40 pots for the experiment. To prevent nutrient deficiencies, a 1:2 Hoagland nutrient solution was applied every two days during the tillering and jointing stages. After 45 days from seedling emergence, one individual plant was selected from each pot for each of the four *Poa* species: *P. crymophila*, *P. pratensis* var. anceps, *P. pratensis*, and *P. botryoides*. This resulted in a total of 40 samples, which were then stored in a refrigerator at -80 °C for total genomic DNA extraction. The individual plants of each species were labeled as follows: L1-L10 for *P. crymophila*, B1-B10 for *P. pratensis* var. anceps, C1-C10 for *P. pratensis*, and H1-H10 for *P. botryoides*. A mixture of 10 individual plant samples from each species were created, and these mixtures were labeled as LD, BJ, CD, and HH, respectively.

To assess cold tolerance across four *Poa* species (*P. crymophila*, *P. pratensis* var. anceps, *P. pratensis*, and *P. botryoides*) and elucidate the physiological and molecular mechanisms underlying cold tolerance in *P. crymophila*, we conducted controlled cold stress treatments at 4 °C for durations of 0, 3, and 6 d, with 25 °C maintained as the control condition. Treatments were initiated on the 45th day post-seedling emergence (Fig. S1). Leaf samples from all species were collected at each treatment interval for comparative physiological analysis, for *P. crymophila*, a comprehensive sampling approach was implemented, collecting leaves (L), stems (S), and roots (R) to facilitate integrated physiological and transcriptomic profiling. Each treatment group contained three biological replicates, with each replicate consisting of five pooled seedlings to ensure adequate biological material. All collected tissues were immediately flash-frozen in liquid nitrogen to preserve molecular integrity and subsequently stored at -80 °C for subsequent analyses.

Determination of indicators and analysis of data

To comprehensively evaluate the cold tolerance of four *Poa* species, the following parameters were measured: relative conductivity (REC) %, malondialdehyde (MDA), proline (Pro), soluble sugar (SS), abscisic acid (ABA), chlorophyll (Chl), fresh weight (FW), dry weight (DW), and the enzyme activities of superoxide dismutase (SOD) and peroxidase (POD). For *P. crymophila*, the physiological responses in different tissues (roots, stems, and leaves) were assessed by measuring MDA, Pro, and the activities of POD, catalase (CAT), and SOD. MDA content was determined using the thiobarbituric acid-reactive substances (TBARS) assay [27], while Pro and SS contents were assessed as described by Wang et al. [1]. Chl content was measured by the acetone extraction method [7], and aboveground FW and DW were determined following the method of Bai et al. [28]. ABA content and the activities of SOD, CAT, and POD were measured according to the manufacturer's instructions for the enzyme assay kits (Shanghai Enzyme-linked Biotechnology Co., Ltd., China).

In the comprehensive evaluation method of cold tolerance, the process involved several steps:

(1). Initially, the raw data for each indicator were used to calculate its cold tolerance coefficient (α) (Table S1), as shown in the formula:

Cold tolerance coefficient (α) = treatment mean / control mean (1).

(2). Subsequently, correlation analyses (Table S2) and principal component analyses (Table S3) were performed on the cold tolerance coefficients of each physiological indicator across the four different *Poa* species. These analyses were conducted using SPSS Statistics 22 in order to ascertain the contribution rate of each indicator (Table S4) to the overall evaluation.

(3). Finally, the seven indicators exhibiting the largest absolute eigenvector values in the first two principal components (PC1 and PC2) were assessed for their association with cold tolerance in the test materials using the fuzzy mathematics-based affiliation function method, as detailed by Xie et al. [29].

Statistical analysis and one-way ANOVA were performed using SPSS Statistics 22. Based on the significance of the results, Tukey's HSD (Tukey's Honestly Significant Difference) was used for multiple comparisons to determine the differences between means ($P < 0.05$). Graphs were also plotted using GraphPad Prism 8.

Total RNA extraction and sequencing

Total RNA was isolated from *P. crymophila* leaves, stems, and roots using a TRIzol-based column kit (Sangon Biotech) [30]. RNA quality was verified through Nanodrop (purity), Qubit 2.0 (concentration), and Agilent 2100 (integrity). Twenty-seven cDNA libraries were constructed with the NEBNext Ultra RNA Library Prep Kit (NEB), indexed for sample identification, and sequenced on an Illumina HiSeq 2000 platform (150 bp paired-end reads; BMKcloud, Beijing). Raw data were processed via BMKCloud (www.biocloud.net) for downstream analysis.

Sequence data processing, de Novo assembly, and annotation

Raw data were obtained after transcriptome sequencing of the library constructed by *P. crymophila*. After filtering raw data, the joint sequences and primer sequences in the raw data were removed, empty sequences and low-quality sequences were screened out, and clean data were obtained for assembly. Unigenes were obtained by de novo transcriptome assembly by Trinity-v2.5.1 (https://github.com/trinityrnaseq/trinityrnaseq/wiki).

The obtained functional gene sequences were aligned by Blastx to protein databases such as NR; Pfam; KOG/COG/eggNOG; Swiss-Prot; KEGG; GO (E-value ≤ $1e^{-5}$). Using KOBAS-v3.0 software (http://kobas.cbi.pku.edu.cn/kobas3) to obtain the results of KEGG Orthology of unigene in KEGG, InterProScan (https://www.ebi.ac.uk/interpro/download/) uses the database integrated by InterPro to analyze the results of GO Orthology of new genes [31]. HMMER-v3.1b2 software (http://hmmer.org/) was used for com-parison with the Pfam database [32] (E-value ≤ $1e^{-10}$).

Analysis of differentially expressed genes

Gene expression levels were quantified using fragments per kilobase per million mapped reads (FPKM). Differential expression analysis between control and cold-treated samples was performed with DESeq (v1.10.1) [33], identifying differentially expressed genes (DEGs) under stringent thresholds: false discovery rate (FDR) < 0.01, adjusted $P < 0.05$, and $|\log2(\text{fold change})| \geq 2$ [18]. The differential expression analysis between the control and cold-treated samples in the *P. crymophila* were compared as; control root (R0) vs. 4 °C treatment for 3 d (R3), R0 vs. 4 °C treatment for 6 d (R6), R3 vs. R6, control shoot (S0) vs. 4 °C treatment for 3 d (S3), S0 vs. 4 °C treatment for 6 d (S6), S3 vs. S6, control leaf (L0) vs. 4 °C treatment for 3 d (L3), L0 vs. 4 °C treatment for 6 d (L6) and L3 vs. L6. Based on functional annotation and enrichment analysis of DEGs, the top 10 DEGs with the highest absolute expression values in each tissue were identified as key DEGs involved in cold response.

Validation analysis of transcriptome data by qRT-PCR

To verify the reliability and accuracy of the RNA-seq data, a random selection of 12 genes from *P. crymophila* was selected for validation by qRT-PCR (Table S5). The same RNA and cDNA were used as for the RNA sequencing experiments. Total RNA was extracted from the 27 samples as described previously and followed the manufacturer's protocol to generate cDNA (Takara, Japan). The qRT-PCR was performed using a ChamQ Universal SYBR qPCR Master Mix kit (Vazyme, Nanjing, China) on a Roche LightCycler480 quantitative PCR. The relative level of gene expression was calculated using the $2^{-\Delta\Delta ct}$ formula [34]. The qRT-PCR analysis included three independent technical repeats with three biological replicates. The beta-actin gene (*PcACTIN*) was used as the internal control gene [35]. Gene-specific primers were designed with DNAMAN software (Lynnon BioSoft, Vandreuil, Quebec, Canada).

Weighted gene co-expression network analysis (WGCNA)

All the DEGs were used for the construction of weighted gene co-expression networks. Filtering the DEGs to remove low-expression genes, DEGs with FPKM > 1 in at least 27 samples were retained. A total of 7,439 DEGs were obtained for WGCNA. The WGCNA assumed that the genetic network followed scale-free networks. The similarity matrix of gene co-expression and gene network

formed the adjacency function. The similarity matrix was transformed into the adjacency matrix and then, the expression correlation coefficient was calculated to construct the gene's hierarchical clustering tree. Modules were divided according to the clustering relationship between genes, and modules with similar expression patterns were merged. Finally, the correlation between phenotypic traits of modules and samples was analyzed, and the hub genes in the network were found by the R language package [30].

Development of EST-SSR markers based on cold tolerance candidate genes

Based on the transcriptome sequencing data of *P. crymophila*, 200 pairs of EST-SSR primers for cold tolerance candidate genes were designed and synthesized according to the gene function annotations. Based on the MISA results and primer design principles, 200 pairs of EST-SSR primers for cold tolerance candidate genes were designed using primer3-v2.3.4. The primers were synthesized by Sangon Biotech (Shanghai) Co., Ltd.

DNA extraction, PCR amplification, primer validation and data analysis

Genomic DNA was extracted from fresh leaf tissues of 40 *Poa* individual and mixed samples of leaves of 4 *Poa* species by adsorption column method using the Plant Genomic DNA Extraction Kit (Tiangen Biochemical Technology Co., Ltd., Beijing, China), and the quality of DNA was determined by using the NanoDrop ND1000 Spectrophotometer, and the DNA that met the conditions was diluted to 25 ng/μL, and stored at -20 °C. The DNA quality was measured by using the NanoDrop ND1000 spectrophotometer. Primer screening was carried out using 10 mixed DNA samples (BJ, CD, HH, LD) of each *Poa* species.

PCR reactions (20 μL total) contained: 10 μL of 2×Reaction Mix, 6.9 μL of ddH_2O, 0.1 μL of Golden DNA polymerase (Beijing Tiangen Biotech Co., Ltd.), 0.5 μL of each of the forward primer and the reverse primer, 2 μL of genomic DNA (25 ng/μL). The PCR amplification program was as follows: pre-denaturation at 94℃ for 3 min, denaturation at 94℃ for 30 s, annealing at 60 – 55℃ for 30 s, and extension at 72℃ for 50 s, with 34 cycles; extension at 72℃ for 7 min, and storage at 4℃. The amplified fragments were separated by 6% denaturing polyacrylamide gel electrophoresis and stained with $AgNO_3$ solution for development. Finally, the gel was photographed and recorded for subsequent analysis. As for the verification of the authenticity of the primers and data analysis, the methods described by Zheng et al. [20] and Zhao et al. [21] were referenced for the operation, respectively. The patterns at all SSR loci were scored for each polymorphic band as 1 for band presence and 0 for band absence. Based on the "0–1" matrix generated from 29 pairs of EST-SSR polymorphic primers, genetic diversity analysis was performed on 40 individuals of four *Poa* species using GenAlEx and POPGENE. Combined with population clustering by STRUCTURE software and genetic similarity analysis using NTSYS software (PCoA-DCENTER module), the genetic structure and variation patterns among samples were elucidated.

Results

Comprehensive evaluation of cold tolerance of four *Poa* species

To evaluate the cold tolerance of different *Poa* species, including *P. crymophila* 'Qinghai', *P. pratensis* var. anceps 'Qinghai', *P. pratensis* 'Qinghai', and *P. botryoides*, physiological indicators were measured after subjecting the plants to cold stress at 4 °C. The results showed that after cold stress treatment, indicators such as REC % (except for *P. crymophila* and *P. botryoides*), MDA content, Pro content, SS content, ABA content, and the activities of SOD and POD increased, while Chl content (except for *P. crymophila* and *P. botryoides*), FW (except for *P. crymophila*), and DW (except for *P. crymophila*) decreased (Fig. 1). Based on principal component analysis (PCA) of 10 indicators (Table S3), 7 indicators of Pro, SS, ABA, FW, Chl, and SOD and POD were finally screened to comprehensively evaluate the cold tolerance using a membership function method revealed that the order of cold tolerance from strong to weak was: *P. crymophila* > *P. botryoides* > *P. pratensis* var. anceps > *P. pratensis* (Table S4 and Table S6). Cluster analysis based on cold tolerance evaluation indexes revealed that *Poa* species with similar cold tolerance tended to cluster together (Fig. S2).

Physiological responses of different tissues of *P. crymophila* under cold stress

Forty-five days old *P. crymophila* seedlings were subjected to cold treatments for 3 and 6 days, respectively. Despite the 4 °C treatments, no observable phenotypic differences were observed compared with control (Fig. S1). However, cold stress resulted in an increase in proline (excluding the roots treated for 3 days) and MDA content, as well as the activity of antioxidant enzymes (SOD, CAT, and POD) in *P. crymophila* (Fig. 2). Proline content in all tissues increased more after 6 days, with a 29.9% rise in roots and 10.6% in leaves compared to 3-day stress. MDA content significantly increased under cold stress, peaking at 6 days (≥ 40% increase). After 6 days, stems and leaves showed a greater MDA increase than roots (Fig. 2). After 3 days of cold treatment, antioxidant enzyme activities of leaves were higher than those in roots (Fig. 2). SOD, CAT, and POD activities of leaves after 3-day stress were 1.92, 2.06, and 1.92 times

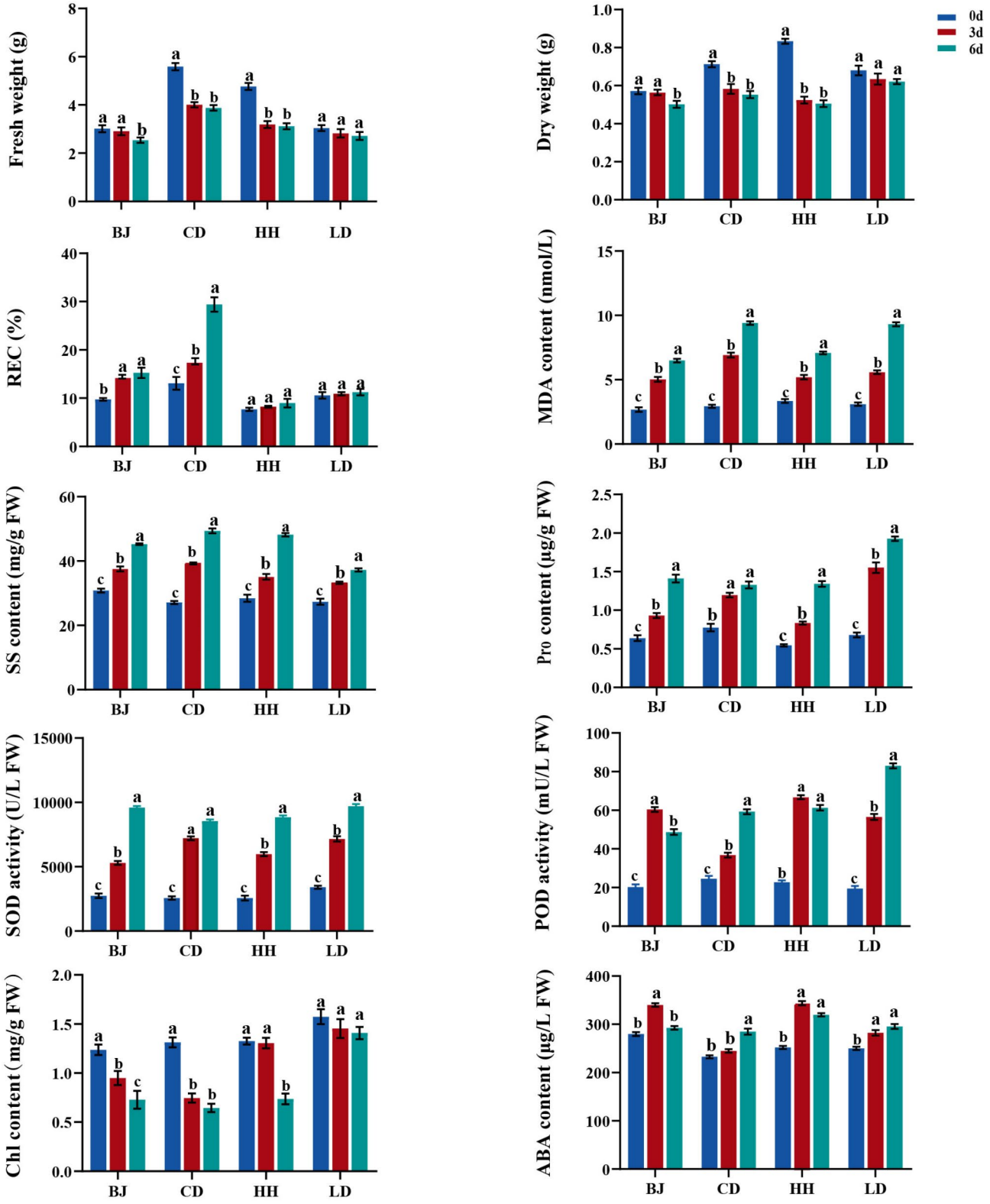

Fig. 1 Changes in indicators of four *Poa* species under cold treatments at 4 °C. BJ, *P. pratensis* var. anceps; CD, *P. pratensis*; HH, *P. botryoides*; LD, *P. crymophila*. FW, fresh weight, DW, dry weight; REC, (relative conductivity); MDA, (malondialdehyde); SS, Soluble sugar; Pro, Proline; SOD, Superoxide dismutase; POD, Peroxidase; Chl, Chlorophyll; ABA, Abscisic acid. All data are presented in the form of mean ± standard error ($n = 3$). Different lowercase letters indicate significant differences between treatments ($P < 0.05$), and the same lowercase letters indicate nonsignificant differences between treatments ($P > 0.05$). The same below

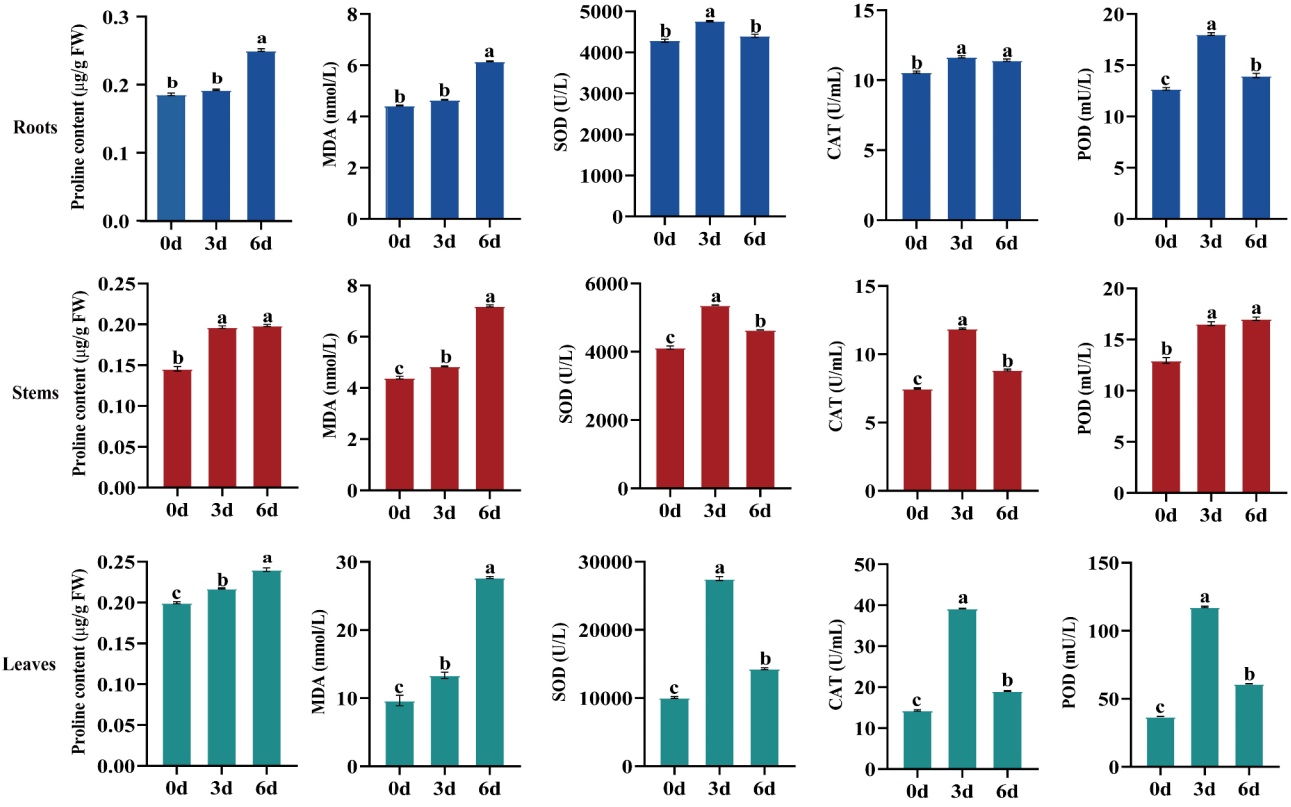

Fig. 2 Analysis of dynamic physiological effects on roots, stems and leaves of *P. crymophila* under cold treatments

than those after 6 days, while activities of roots were 1.08, 1.02, and 1.29 times higher after 3 days than 6 days.

Transcriptome assembly and annotation

A total of 27 samples were employed to construct the cDNA library. After trimming, 193.28 Gb databases were retrieved, or approximately 5.99 Gb per sample (three biological replicates) (Table S7). Furthermore, we obtained approximately 20.03 to 29.68 million clean reads per library, mapped at a ratio of 65.45%. The number of bases ranged from 5.99 billion to 8.85 billion. The Q3 base percentage was >92.69%. The GC content was approximately 55.25% (Table S7). These results suggested that the sequencing output and high-quality reads were adequate for further analysis.

After de novo assembly of high-quality sequences by Trinity software, a total of 1,868,509 transcripts and 53,893 unigenes were generated with average lengths of 1108.27 bp and 2243.7 bp respectively, and the N50 lengths of 1681 bp and 2941 bp respectively (Table S8). The size-distribution analysis showed that the lengths of 41,330 (76.69%) unigenes were greater than 1000 bp (Table S8). These results demonstrated the effectiveness of Illumina sequencing in rapidly capturing a large portion of the transcriptome. Further, 46,542 (86.36%) of the unigenes were successfully annotated in nine databases (Table S9).

Currently, homologous species matched results in Nr database showed that the top 8 mostly annotated plants belong to Poaceae species, and Triticum aestivum (10,398, 23.26%) was the best match for *P. crymophila*, followed by *Brachypodium distachyon* (7,328, 16.39%) and *Aegilops tauschii* (6,662, 14.90%) (Fig. S3A). In addition, the E-value distribution and similarity statistics of the annotated unigenes showed that 89.36% of the unigenes had an E-value less than $1e^{-30}$ and had high homology (Fig. S3B), unigenes with a similarity greater than 60% and greater than 80% accounted for 86.93% and 58.91%, respectively, indicating that the unigenes annotation information of *P. crymophila* has good reliability (Fig. S3C).

Identification and analysis of DEGs

A total of 22,233 DEGs were identified in all tissues under cold treatments. The number of DEGs in leaves was three times higher than in roots and 1.5 times higher than in stems (14942, 4434, and 8793 DEGs, respectively) (Fig. 3A). Among them, 1975, 4892, and 9894 DEGs were found to be unique to roots, stems, and leaves, respectively. These results indicated that cold-induced transcriptome responses were largely tissue-specific. Notably,

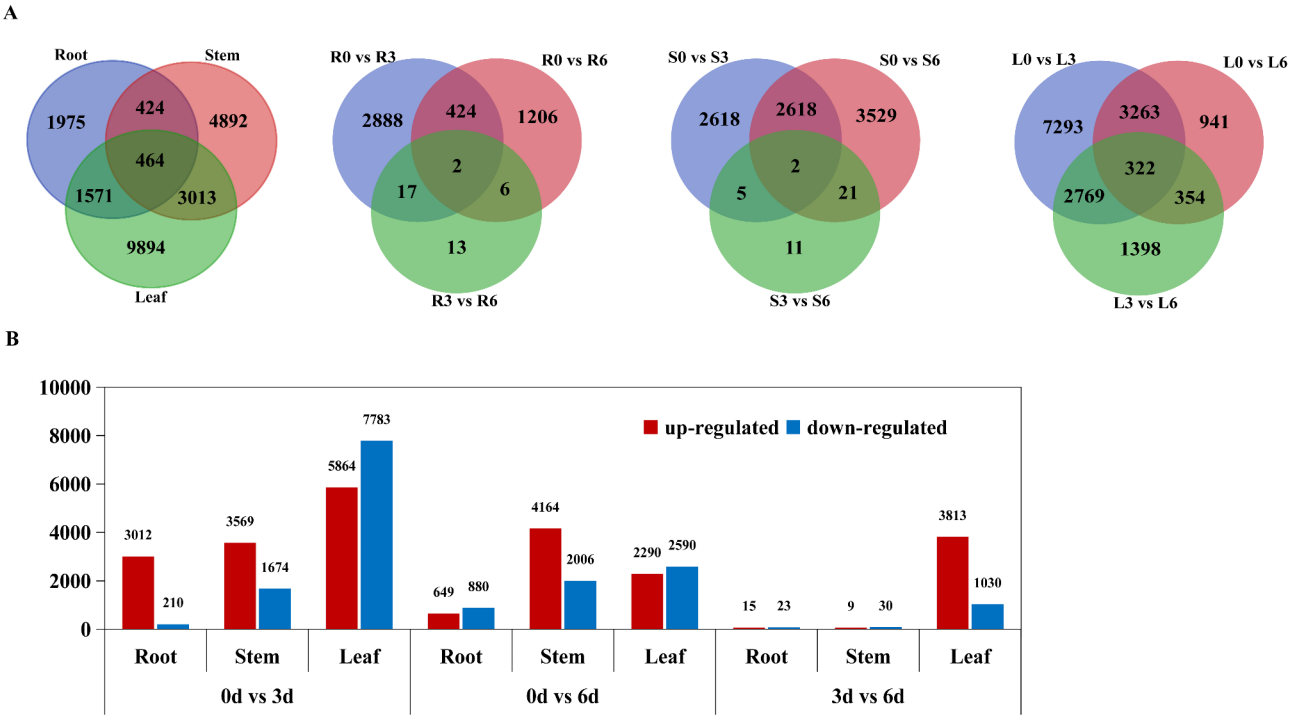

Fig. 3 Summary of differentially expressed genes (DEGs). (**A**) Summary of the numbers of roots, stems, and leaves DEGs under cold treatments. The differential expression analysis between the control/cold conditions in the *P. crymophila* were compared as: control root (R0) vs. 4 °C treatment for 3 d (R3), R0 vs. 4 °C treatment for 6 d (R6), R3 vs. R6, control shoot (S0) vs. 4 °C treatment for 3 d (S3), S0 vs. 4 °C treatment for 6 d (S6), S3 vs. S6, control leaf (L0) vs. 4 °C treatment for 3 d (L3), L0 vs. 4 °C treatment for 6 d (L6) and L3 vs. L6. (**B**) The number of genes whose expression is differentially regulated under cold treatments, 4 °C treatment for 0 d (0d) vs. 4 °C treatment for 3 d (3d), 4 °C treatment for 0 d (0d) vs. 4 °C treatment for 6 d (6d), 3d vs. 6d

464 genes were commonly expressed in three tissues (Fig. 3A). The comparison of different treatment time points found more DEGs, 2888 and 7293 DEGs, were specifically expressed between R0 vs. R3 and L0 vs. L3, respectively (Fig. 3A). Moreover, it was found that more up-regulated DEGs were obtained in roots (3012 DEGs) and leaves (5864 DEGs) under 3 days of cold treatment than under 6 days of cold treatment (Fig. 3B). These results suggest that more transcripts responded to cold stress during 3 days than during 6 days. To obtain an overall picture of the impact of cold stress on transcriptional profiling, the expression patterns of all DEGs identified in the three tissues at the different time points were clustered together. Six expression patterns were identified in each tissue ($P < 0.05$) (Fig. S4). The results showed that the expression of many more DEGs was up-regulated in leaves under cold stress, followed by stems and roots.

Experimental validation

To validate the RNA sequencing (RNA-seq) data of the present study, the expression profiles of a subset of 12 DEGs involved in oxidation-reduction, membrane components, and hormone signal transduction were selected for qRT-PCR assays. The variation trends and errors of these 12 DEGs at different treatment points showed a high degree of consistency with the change tendency of the transcript FPKM values (Fig. S5). The coefficients of determination obtained by linear regression analysis between the qRT-PCR and transcriptome data of the roots, stem, and leaves were $R^2 = 0.7$, $R^2 = 0.78$, and $R^2 = 0.85$, respectively, and the correlations were positive (Fig. S6). The high congruence between the RNA-seq and qRT-PCR results indicated the reliability of the gene expression values in our experiment.

GO and KEGG enrichment analysis of DEGs

To further determine the coordinated response mechanisms in the roots, stems, and leaves of *P. crymophila* seedlings under cold stress, GO category enrichment analysis was applied to determine the function of the DEGs expressed under cold stress. According to the *P*-value and number of DEGs associated with GO terms, the top 25 significantly enriched GO terms were selected and further analyzed. GO results showed that DEGs were most enriched in the "response to stimulus" category in roots and stems under cold stress, and most DEGs were up-regulated (Fig. 4A, B and Table S10). In addition, categories associated with water response ("water transmembrane transporter activity", "water channel activity", and "water transport") and photosynthesis ("chloroplast",

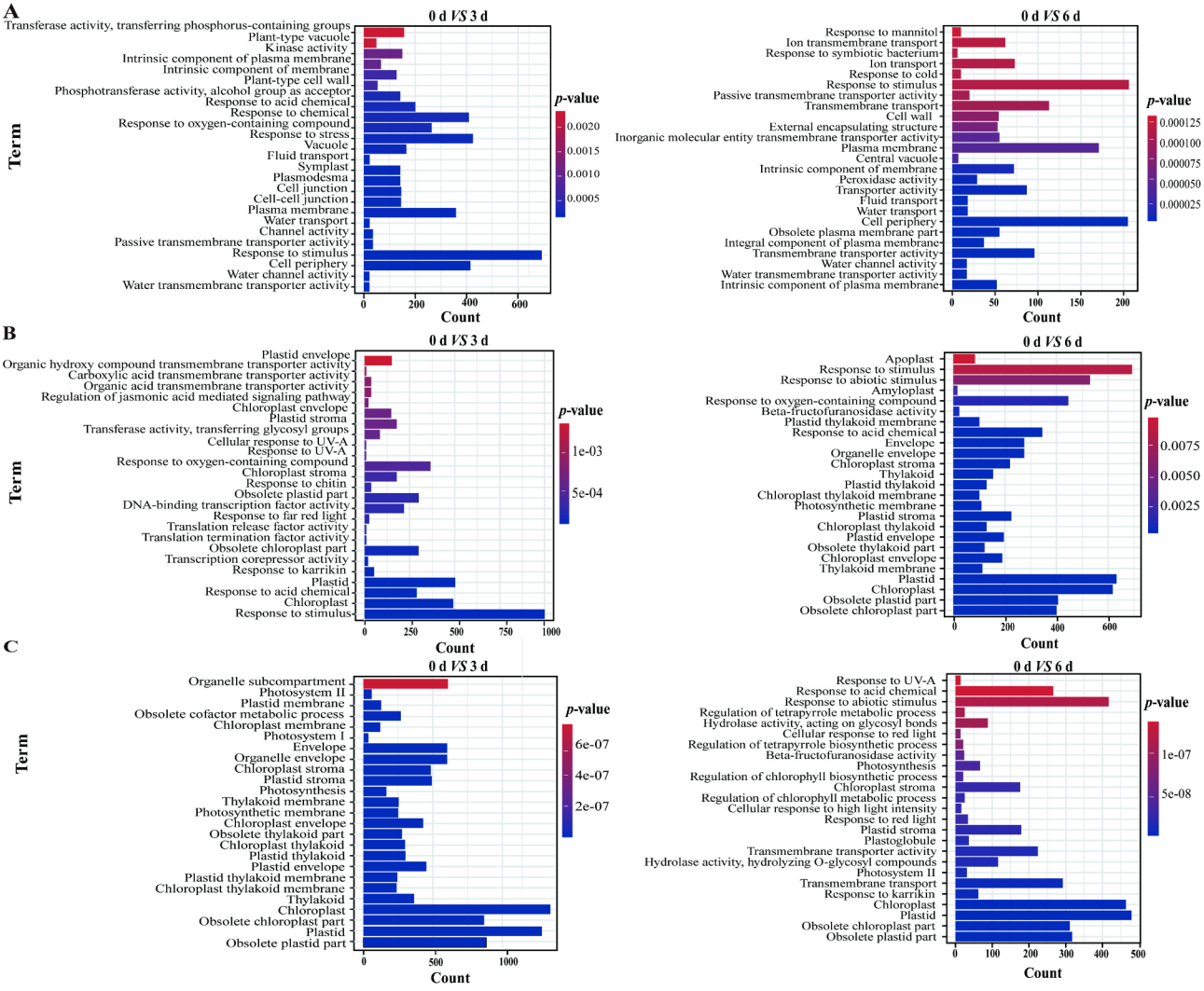

Fig. 4 GO enrichment analysis of DEGs in *P. crymophila* under 3 and 6 days of cold stress. (**A**) roots. (**B**) stems. (**C**) leaves. For more detailed information about GO term, please refer to Table S10

"plastid", "obsolete chloroplast part", "obsolete plastid part", "chloroplast stroma", "chloroplast envelope", "plastid stroma") were significantly enriched in roots and stems, respectively. For leaves, inversely, large numbers of DEGs were significantly enriched in photosynthesis-related categories ("chloroplast", "obsolete chloroplast part", "photosystem II", "photosynthesis", "plastid stroma", "chloroplast stroma", and "plastid") under cold stress, and the DEGs involved with these categories were predominantly down-regulate (Fig. 4C and Table S10).

The DEGs were further annotated to the reference pathways in the KEGG database to explore the key biological pathways in response to cold stress in *P. crymophila*, and the top 20 pathways were screened as the most enriched pathways. The DEGs of the root were significantly enriched in the "phenylpropanoid biosynthesis" both in 3 days and 6 days of cold stress, and most of them were up-regulated (Fig. 5A and Table S11). Furthermore, it was found that most of the DEGs were significantly enriched in the "MAPK signaling pathway-plant" (3 days), "plant hormone signal transduction" (6 days) pathways and were up-regulated in roots (Fig. 5A and Table S11). The DEGs involved in the "Circadian rhythm-plant" (39 DEGs) and "photosynthesis" (41 DEGs) pathways were significantly enriched in stems, and were up-regulated (Fig. 5B and Table S11). For leaves, "photosynthesis" and "starch and sucrose metabolism", "galactose metabolism", "circadian rhythm-plant", "glutathione metabolism", "arginine and proline metabolism", "biosynthesis of amino acids" pathways were significantly enriched both at 3 and 6 days of cold stress (Fig. 5C). Most of the DEGs involved in the "photosynthesis" pathway were down-regulated in leaves while in "circadian rhythm-plant" pathway were up-regulated (Table S11). Notably, all DEGs involved in "photosynthesis-antenna proteins" (33 DEGs) were significantly down-regulated after 3 days of cold stress (Table S11). In addition, "starch and sucrose metabolism" and "galactose metabolism" pathways were significantly

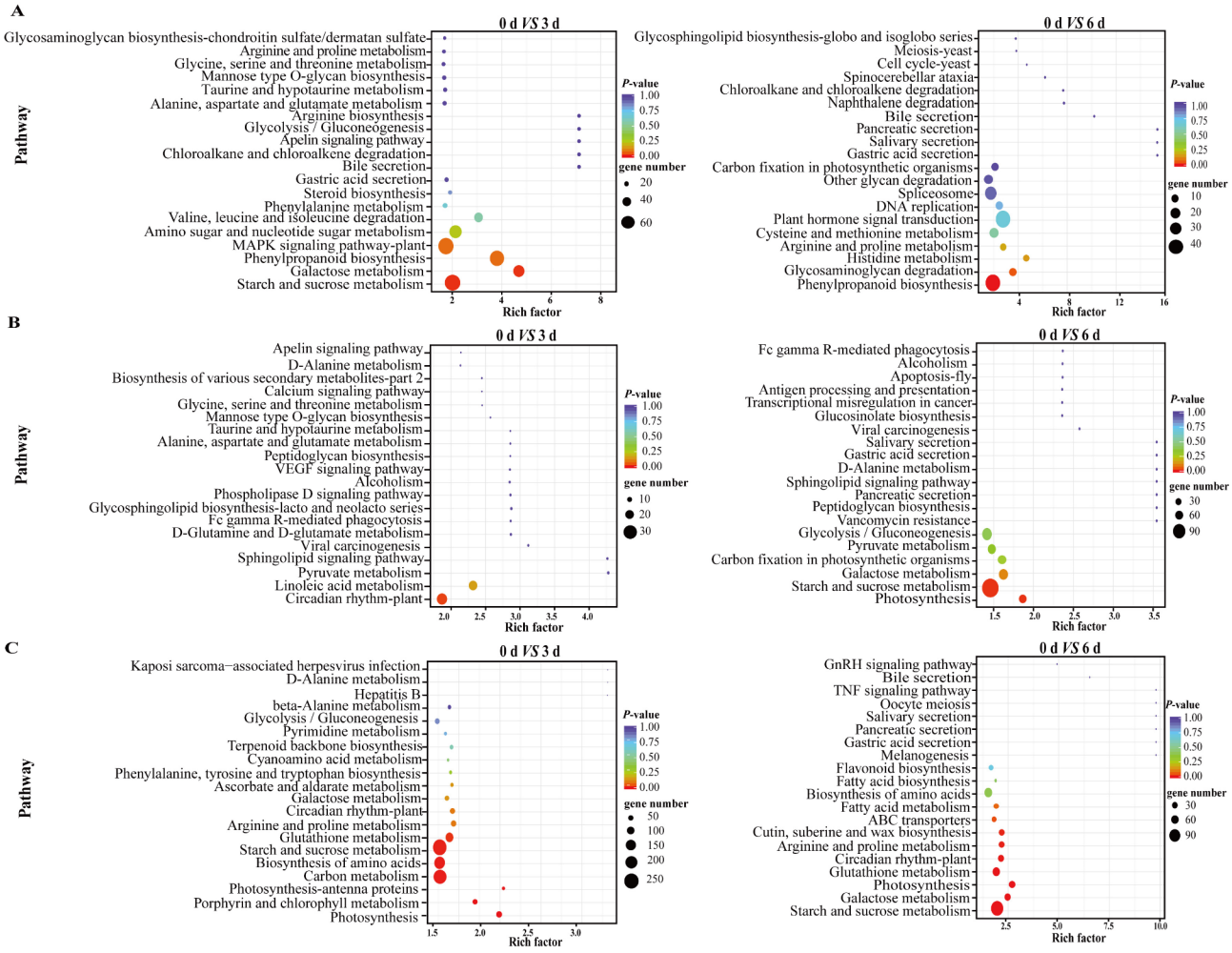

Fig. 5 KEGG pathway enrichment analysis of DEGs in *P. crymophila* under 3 and 6 days of cold stress. (**A**) roots. (**B**) stems. (**C**) leaves. For more detailed information about KEGG pathway, please refer to Table S11

enriched in roots (3 days), stems (6 days), and leaves (both at 3 and 6 days) (Fig. 5).

Identification of key DEGs involved in cold responses

Based on gene functional annotation and enrichment analysis, 392 candidate genes involved in cold tolerance mechanisms in *P. crymophila* were screened (Fig. 6). They were TFs (52 DEGs), CBF pathway (70 DEGs), Ca^{2+} signaling (60 DEGs), hormone signaling (61 DEGs), ROS scavenging system (76 DEGs), photosynthesis and biological clock (49 DEGs) and plant carbohydrate metabolism pathway (24 DEGs). Further analysis of the differentially expressed gene sets for comparison revealed six C2C2-Dof and three MADS-box TFs were identified (Fig. 6A), twenty-three COR DEGs identified in the CBF pathway (Fig. 6B), five CNGC, seven GLR, nine CAMTA and five CBL DEGs identified in Ca^{2+} signaling (Fig. 6C), eleven PP2C DEGs found in hormone signaling associated with ABA (Fig. 6D), three SOD, three CAT, four POD, fifteen GST, eight MDAR DEGs found in ROS scavenging system (Fig. 6E), nine PRR, LHY, and three GI DEGs found in photosynthesis and circadian clock (Fig. 6F), and fifteen DEGs were involved in starch and sucrose metabolism and galactose metabolism pathways (Fig. 6G), which were mainly up-regulated in stems and leaves. five bHLH and ten WRKY TFs were identified (Fig. 6A), ten CRPK and six ZAT DEGs were identified in the CBF pathway (Fig. 6B), four EIN3 and four CYP and five REF DEGs were identified in hormone signaling related to ABA and ETH (Fig. 6D), and three PSI and fifteen PAP (photosynthesis-antenna protein) DEGs were identified in photosynthesis (Fig. 6F), which were mainly up-regulated in stems and leaves.

WGCNA and identification of hub genes

Following the screening of low-expressed genes, 7,439 DEGs were selected for WGCNA. To construct a scale-free network with biological relevance, a soft threshold power of 16 was chosen at a squared correlation coefficient of 0.9 to define the adjacency matrix (Fig. 7A). Using the DynamicTreeCut algorithm, with a minimum of 30 module genes and a maximum module distance of 0.25, gene modules were generated and highly similar

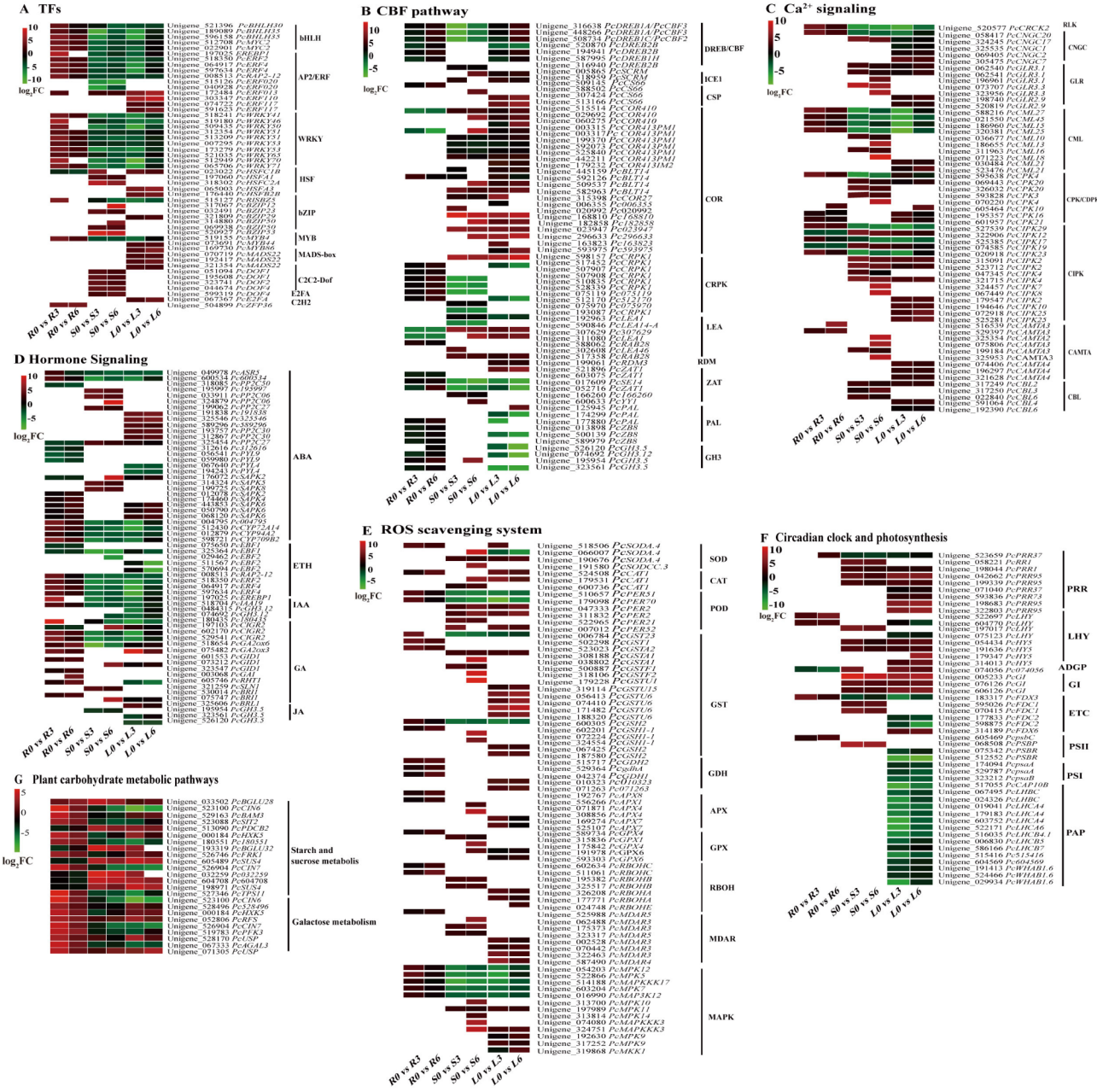

Fig. 6 Heat map expression of candidate genes for cold tolerance in *P. crymophila*. (**A**) TFs. (**B**) CBF pathway. (**C**) Ca^{2+} signaling. (**D**) Hormone signaling. (**E**) ROS scavenging system. (**F**) Circadian clock and photosynthesis. (**G**) Plant carbohydrate metabolic pathways

ones were merged (Fig. 7B, C). Ultimately, 17 gene modules were obtained (Fig. 7D). The results showed that antioxidant enzyme activities (SOD, CAT, POD) strongly positively correlated ($r > 0.9$) with the brown module and negatively correlated ($r < -0.6$) with the salmon module.

GO and KEGG enrichment analyses were conducted on the brown and salmon modules, and co-expression networks were visualized (Fig. 8). In the brown module, "response to stimulus" (235 DEGs) and "Circadian rhythm-plant" pathway were the top-enriched GO categories and KEGG pathways, respectively (Fig. 8A, B). In the salmon module, "endomembrane system" (32 DEGs) and "Phagosome" were the top-enriched GO categories and KEGG pathways, respectively (Fig. 8A, B). The first six hub genes in the brown module were identified: *Unigene_600094*(*PcERF*), *Unigene_023873* (*PcBLH1*), *Unigene_019968* (*PcABCC2*), *Unigene_513952* (*PcUGT73C1*), *Unigene_325532* (*PcFTSH1*) and *Unigene_075399* (*PcABC1K7*). The first three hub genes in the salmon module were identified as *Unigene_530024* (*PcCTR1*), *Unigene_605651* (*PcCARB*) and *Unigene_595662* (*PcGlCAT14A*), these genes were

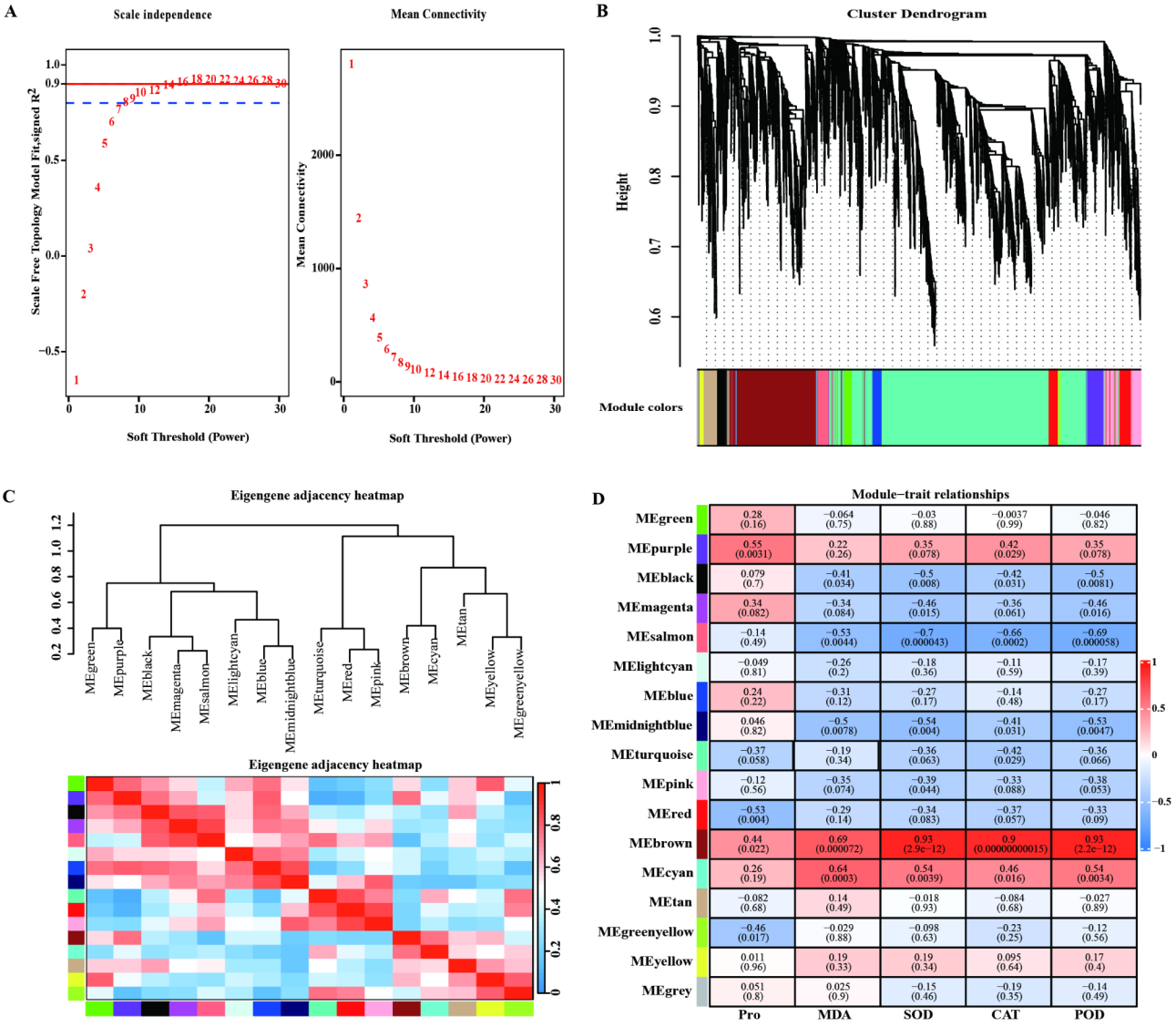

Fig. 7 WGCNA associated with cold response. (**A**) Scale independence and mean connectivity. (**B**) Gene cluster tree. (**C**) Module diagram. (**D**) Correlation heatmap between modules and traits

mostly up-regulated (Fig. 8C, Table S12 and Fig. S7). The nine hub genes with higher connectivity within the module correlate better with the activity of antioxidant enzymes. This provided insight into the cold-responsive genes of *P. crymophila* for subsequent research.

Development of candidate gene-based EST-SSR markers and application in genetic diversity analysis

To facilitate molecular marker-assisted selection for cold tolerance in *P. crymophila*, 12,972 SSR loci were identified from 53,893 unigenes, distributed among 10,766 unigenes, accounting for 19.98% of all sequences (Table S13). Based on candidate cold-resistant genes, 200 molecular markers were developed and screened for polymorphisms. A total of 29 polymorphic molecular markers involved in the ROS scavenging system, hormones regulation, calcium regulation, photosynthesis and transcription factors (TFs) were used for genetic diversity analysis and cold tolerance screening of 40 individual plants (Table S14). The polymorphic information content (PIC) of the 29 pairs of primers ranged from 0.22 to 0.42, with an average of 0.35 (Table S14).

Based on the gel electrophoresis results, primers P37 (*PcGA2ox3*) and P148 (*PcERF013*) with clear bands and good polymorphism were selected for further analysis, and it was found that the markers P37 and P148 could distinguish *P. crymophila* (LD). A distinct 150 bp amplification product was detected by P37 marker in *P. botryoides* (HH), *P. pratensis* var. anceps (BJ), and *P. pratensis* (CD) genotypes, while the LD genotype showed no amplification at this target size (Fig. S8A). The P148 marker revealed differential banding patterns: amplification products in the 150–200 bp range

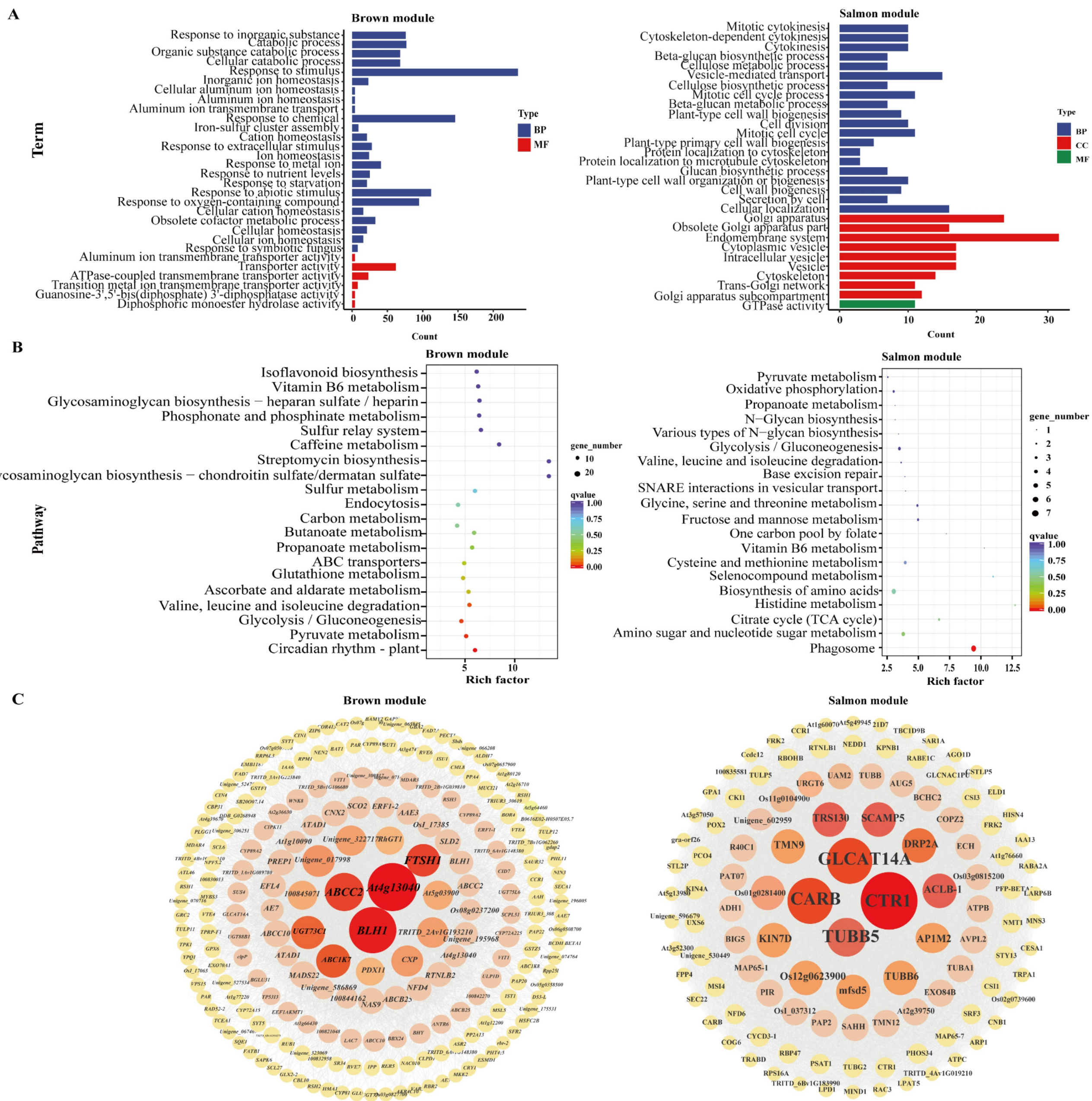

Fig. 8 Analysis of DEGs for brown and salmon modules. (**A**) GO enrichment analysis. (**B**) KEGG pathway enrichment analysis of DEGs in brown module and salmon module. (**C**) Co-expression network visualization of brown and salmon module

were observed in BJ and HH genotypes; an 80 bp fragment was consistently amplified in BJ, CD, and HH; LD exhibited null amplification at both target regions (150–200 bp and 80 bp) (Fig. S8B). To verify the authenticity of the developed EST-SSR markers, 20 *Poa* sample DNAs were amplified with these two EST-SSR markers, and the amplified products were sequenced. According to the sequencing results of PCR amplification products of primer P37, three base repeat types, (CCA)2, (CCA)3, and (CCA)5, were found in different *Poa* species genotypes (Fig. S9A). Three base repeat types, (AGC)2, (AGC)3 and (AGC)3, were found in primer P148 for different *Poa* species (Fig. S9A). To verify that the variation in the number of repeats of the SSR sequences was responsible for the marker polymorphisms found in the four *Poa* species, the sequences of PCR products amplified by primers P37 and P148 were compared in detail. The results of the analysis showed the presence of base mutations in these sequences among the different *Poa* species (Fig. S9B).

The results of the UPGMA unweighted group average method, with a genetic similarity coefficient of 0.70, indicated that the 40 *Poa* individuals were clustered into three major groups (Fig. 9A). This clustering was

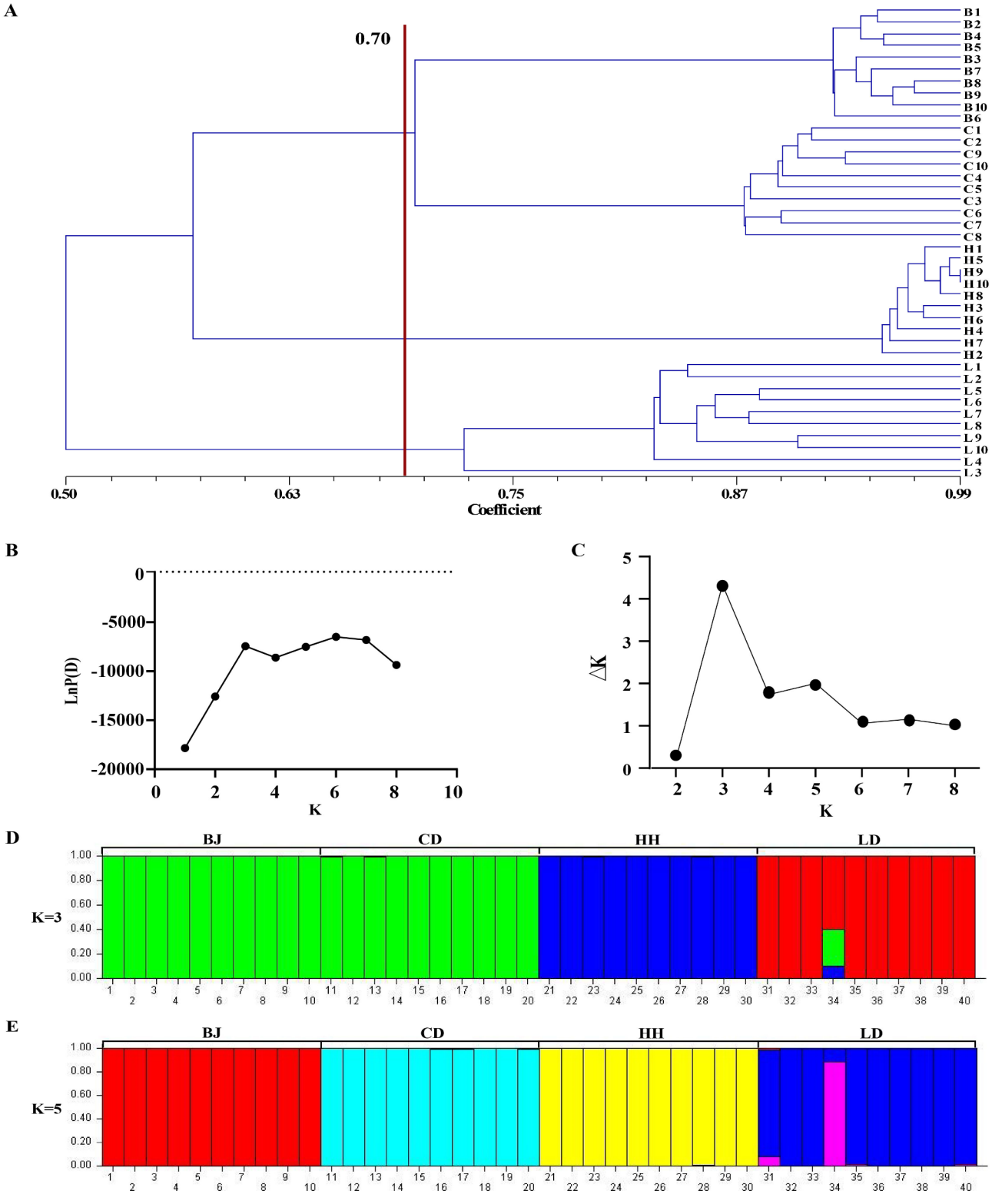

Fig. 9 Genetic structure of four *Poa* populations analyzed based on 29 EST-SSR markers. (**A**) Cluster analysis grouped 40 genotypes by UPGMA dendrogram (genetic similarity coefficient = 0.70): BJ (*P. pratensis* var. *anceps*; B1-B10), CD (*P. pratensis*; C1-C10), HH (*P. botryoides*; H1-H10), LD (*P. crymophila*; L1-L10). (**B**) Mean LnP(D) values for 20 runs at each K value. (**C**) Optimal hierarchical structure for K = 3 was determined using the largest ΔK value; (**D**-**E**) Population stratification patterns at *K* = 3 versus *K* = 5, with vertical coordinates indicate the affiliation coefficients for each genotype (1–40: BJ [1–10], CD [11–20], HH [21–30], LD [31–40]; color-coded by population)

consistent with the results of the STRUCTURE analysis (K = 3), which demonstrated that *Poa* species with similar cold tolerance were grouped together (CD and BJ) (Fig. 9C, D). This shows that there is cross-clustering between the BJ and CD populations. According to results of STRUCTURE analysis, we also found that the 34th individual plant (L4) of LD is closely genetically related to CD and BJ, and according to the sequence comparison of the PCR products amplified by the two primers (P37 and P148) (Fig. S9B and Fig. 9D), it was found that the sequence of the PCR product of the individual plant of L4 is indeed the same as that of the PCR products amplified by BJ and HH. When K = 5, the four populations BJ (red), CD (turquoise), HH (yellow), and LD (blue) can be clearly distinguished, whereas LD's individual plant 34 (L4), which is pink, is the furthest away from the genetic background of the other individual plants (Fig. 9E). Therefore, EST-SSR molecular markers based on cold tolerance candidate genes have the potential to distinguish *Poa* genotypes with different cold tolerance.

Discussion

Comprehensive evaluation of cold tolerance of *Poa* species

The cold tolerance in plants is an extremely complex trait, and different *Poa* species may use different mechanisms to cope with cold stress [36]. In this study, it was found that the fresh weight, dry weight and chlorophyll content of all *Poa* species generally decreased ($\alpha < 1$) under cold treatments, however, in terms of other indexes, the coefficient of cold hardiness showed a tendency to increase ($\alpha > 1$) under cold conditions, and the performances of different species were differentiated, and there were also significant differences between different physiological indexes even in the same species (Fig. 1; Table S1). In order to reveal the response mechanism of *Poa* species to cold stress more comprehensively and improve the accuracy of tolerance evaluation, it is necessary to utilize several important physiological indexes to comprehensively evaluate their cold tolerance. The affiliation function, as a comprehensive resistance evaluation method based on multiple indicators, has been used for resistance evaluation in rice, wheat and cotton [37–39]. Sun et al. [39]. combined PCA to screen for key drought indicators associated with drought tolerance and screened two cotton materials for higher drought tolerance. In this study, we comprehensively evaluated the cold tolerance of the four *Poa* species by combining correlation analysis, PCA and cluster analysis, and found that *P. crymophila* was the most cold-resistant (Table S16), which tended to cluster with *P. botryoides*, while *P. pratensis* var. anceps and *P. pratensis*, which were less cold-resistant, tended to cluster together (Fig. S2). *P. crymophila* demonstrated superior cold tolerance relative to congeneric *Poa* species via coordinated physiological mechanisms: elevated proline levels supporting osmotic adjustment, maintained chlorophyll content ensuring photosynthetic stability, enhanced SOD/POD activity facilitating reactive oxygen species (ROS) scavenging, and decreased relative electrolyte leakage (REC) indicating membrane integrity preservation (Fig. 1). These adaptive responses collectively promote sustained growth under cold conditions (Fig. S1). Based on this result, we chose *P. crymophila* for the next physiological and transcriptomic analysis.

Physiological changes in *P. crymophila* responding to cold stress

When plants encounter cold stress, their physiology or cells will be disturbed, such as cell membrane permeability, membrane lipid peroxidation, plant protection enzyme activity and photosynthesis [12]. Plants can accumulate more compatible substances to mitigate damage caused by cold stress, such as proline, which acts as an osmoprotectant and allows plants to tolerate cold stress [26, 40]. Cold stress leads to overproduction of ROS in the cells that damages various biological molecules and causes membrane lipid peroxidation [15, 40]. To maintain ROS homeostasis plants have evolved defensive mechanisms composed of enzymatic and non-enzymatic components such as SOD, CAT, and POD [2, 11, 12]. In *P. crymophila*, the proline content, MDA content, and antioxidant enzyme activity increased in all three tissues under cold stress. Furthermore, the MDA content and antioxidant enzyme activity in stems and leaves exceeded those of roots during each stress period (Fig. 2). These observations collectively led to the hypothesis that the aboveground tissues of *P. crymophila* exhibit heightened responsiveness to initial cold signals and possess superior adaptive mechanisms for rapidly mitigating cold stress. Nevertheless, the tissue-specific transduction pathways of cryogenic signals under extreme subzero conditions (sub-zero temperature) and their subsequent molecular regulation remain an open question worthy of rigorous investigation.

TFs involved in the cold stress response

TFs play important regulators of various biological and molecular functions in plants that activate the downstream gene transcripts to display responses against cold stresses [23, 41, 42]. For instance, *OsERF096* modulates IAA accumulation and signaling in regulating cold tolerance of rice [42], the japonica version of *bZIP73* interacts with *bZIP71* to regulate ABA levels and ROS homeostasis for cold acclimation in japonica rice [43]. In addition, differences in the types and levels of TFs expression can significantly affect the ability of plants to adapt to cold stress. It has been shown that *E. nutans* specifically expresses bHLH, bZIP, C2H2, WRKY, and MYB TFs at the early stage of cold stress [25], and that the temporal

specificity in the expression levels of the TFs enhances the cold tolerance of the plant [7]. In the present study, the main differentially expressed TFs in *P. crymophila* at 3 days of cold treatment were AP2/ERF, bHLH, WRKY, MYB, bZIP, C2H2, and HSF TFs. Additionally, MADS-box, C2C2-Dof, and E2FA TFs were up-regulated only in the stems or leaves (Fig. 6A). Thus, the tissue-specific expression patterns of particular TFs and their differential regulation under varying cold stress conditions may critically determine plant cold tolerance enhancement.

Role of ICE-CBF-COR in the cold response

The ICE-CBF-COR signaling pathway has been the best characterized cold stress signaling pathway [8, 44]. In Arabidopsis, the cold-induced *AtCBF* activates the expression of *CORs*, which in turn initiates a variety of mechanisms such as membrane stabilization and scavenging of ROS to mitigate cold damage [5, 45]. LEAs are antioxidants and stabilizers of membranes and proteins, and the expression of *AtCBF3/AtDREB1A* improves cold tolerance in Arabidopsis by increasing the levels of *LEAs* [45, 46]. *CSPs* were highly expressed in the cold-resistant plants, and it has also been reported that *CSPs* were up-regulated by the *CBFs* in response to cold stress in Arabidopsis [47]. In this study, the ICE-CBF-COR signaling pathway also plays an important role in the response to cold stress in *P. crymophila* (Fig. 6B). In *P. crymophila*, six cold-responsive genes (*PcLEA1*, *PcLEA14-A*, *PcCOR413PM*, *PcCOR413IM2*, *PcCOR410*, and *PcBLT14*) exhibited tissue-specific expression in stems and leaves, where they conferred enhanced cold tolerance through ROS scavenging, thereby alleviating cold-induced cellular damage (Figs. 2 and 6B). Notably, transcriptional regulators *PcICE1* and *PcCSP* showed significantly higher expression levels in aerial tissues than in roots, suggesting their specialized role in orchestrating downstream defense mechanisms that potentiate cold stress adaptation in aboveground organs.

Role of Ca^{2+} signaling, hormone signaling, and ROS scavenging system in the cold response

Ca^{2+}, hormones and ROS act as signaling molecules that are involve in response to various stresses [2, 5]. In *P. crymophila*, many genes encoding calcium-related proteins responding to cold stress, including Ca^{2+} channel proteins CNGC and GLR, Ca^{2+} sensors CML, CBL, CPK/CDPK, CIPK, Ca^{2+}-binding transcription factor CAMTA (Fig. 6C). To ensure the normal transmission of cold stress signals with the fluctuation of Ca^{2+}concentration, *P. crymophila* has a higher expression level of the calcium channel proteins [23]. Ca^{2+} sensor protein senses temperature changes through monitoring intracellular calcium levels, interprets this signal as stress and passes it downstream, acting as a master switch to regulate various stress genes that confer cold tolerance [8, 23]. *CAMTA* has CaM-binding activity and contributes to the cold induction of CBF genes, when the *CAMTA3* binds to the *CBF2* promoter, *CBF2* is activated, which increases the cold tolerance of plants [2]. Therefore, it was speculated that Ca^{2+} signaling pathway components in *P. crymophila* exhibits tissue-specific prioritization, with leaf and stem tissues demonstrating earlier component activation than roots (Fig. 6C). This spatial-temporal regulation likely enhances cold signal perception in aerial organs, enabling accelerated initiation of cold adaptation mechanisms prior to root system responses.

IAA, GA and BR are growth-promoting hormones that promote cell elongation and division, ABA, ETH and JA often act as stress signaling and play an important role in regulating plant tolerance to abiotic stresses [48–50]. GH3(Gretchen Hagen 3) proteins are usually involved in regulating the synthesis and accumulation of JA and IAA [51, 52]. In rice, overexpression of *OsGH3-2* inhibited the accumulation of free IAA, which leads to the enhancement of ROS scavenging capacity and ultimately promoted cold tolerance [51]. Both GA metabolism and signaling can affect the cold stress responses of plants, and studies have shown that CBF upregulates multiple genes involved in GA metabolism (*GA2ox3*, *GA2ox6*, and *GA2ox9*) and signaling (RGL3) under cold stress, thereby reducing bioactive GA levels [50]. The activity of DELLA is central to GA signaling, DELLA (*RHT1*) proteins interact with the GA receptors, alleviating DELLA repression on GA signaling [48]. Moreover, BR was able to enhance the expression of *AtCBF1* and *AtCOR47*, which ultimately improved cold tolerance in Arabidopsis [53]. In response to cold, reduced expression of *MwBRH1*(*Brassinosteroid response 1*) and increased expression of *MwBRI1* (*brassinosteroid LRR receptor kinase BRI1*) activate BR signaling in *Magnolia wufengensis* [54]. Therefore, it could suggest that *P. crymophila* enhances cold tolerance through coordinated phytohormone regulation: decreased levels of IAA, GA, and BR in conjunction with suppressed expression of *GH3* genes (*PcEBF1* and *PcEBF2*), which reduces IAA catabolism, while elevating JA accumulation in root and stem tissues (Fig. 6D).

Studies have shown that ABA is a core regulator of cold stress signaling and plays a crucial role in CBF-dependent pathway [50, 55]. *Abscisic acid insensitive 1* (*ABI1*), *abscisic acid insensitive 2* (*ABI2*) and *Hypersensitive* to *Abscisic acid 1* (*HAB1*) have been shown to interact with ABA re-ceptors *PYR/PYLs* (*Pyrabactin-resistant/PYR1-like proteins*) to regulate *SNF1-Related Protein Kinase 2* (*SnRK2s*) and *Protein phosphatase 2 C* (*PP2Cs*) [48, 50]. In this study, *P. crymophila* may promote PP2C (*PcPP2C06*, *PcPP2C27*, *PcPP2C30*) and SnRK2 DEGs (*PcSAPK2*, *PcSAPK4*, *PcSAPK5*, *PcSAPK6*, *PcSAPK8*) expression through the downregulation of PYR/PYL DEGs (*PcPYL4* and *PcPYL9*) in the ABA

regulatory pathway, thereby improving cold tolerance (Fig. 6D). Furthermore, *ethylene-insensitive 3* (*EIN3*) acts as an antagonist in the ETH signaling pathway, modulating cold acclimation by inhibiting *CBFs* [12, 48]. Under cold stress, ABA, and JA hormones can induce the expression of ERF genes, and *ERFs* bind to GCC box and DRE elements, conferring cold stress tolerance in *A. thaliana* and *T. aestivum* [12]. These DEGs are vital for the cold stress response in *P. crymophila*, and reducing *EIN3* (*PcEBF1* and *PcEBF2*) can relieve the inhibition of the CBF pathway, thereby elevating *P. crymophila*'s cold tolerance.

ROS can function as a cold stress marker that impacts downstream gene expression. It may be due to protein denaturation, nucleic acid mutations, and cellular damage [56, 57]. It has been found that cold stress induces SOD, POD, and CAT activities to scavenge ROS, thereby enhancing cold tolerance in plants [56, 57]. In this study, we found that cold stress-induced upregulation of antioxidant biosynthesis genes encoding SOD, POD, and CAT in *P. crymophila*, with strongest differential expression observed in stems and leaves (Fig. 6E). This tissue-specific transcriptional activation showed positive correlation with corresponding enzymatic activity elevations, demonstrating cold-responsive reinforcement of the ROS-scavenging system (Fig. 2). In addition, APX, GSH and GPX, as the most important peroxidases in H_2O_2 detoxification, play an important role in scavenging ROS to enhance cold tolerance in plants [8, 56]. In winter wheat *Dn1* [41] and *Capsicum annuum* L [58]., the higher activities of RBOH, DHAR and MDHAR enzymes have a significant effect on alleviating the symptoms of cold stress. In summary, these enzymes of the ROS scavenging system protect cells from damage and ensure normal life under stress, which is also the strategy of *P. crymophila* cold adaptation.

The MAPK cascade is a universal signal transduction module, including MAPK, MAPKK/MKK/MMK, and MAPKKK/MEKK, lies downstream of ROS, Ca^{2+} and hormones, and play vital roles in plant responses to cold stress [59–61]. The overexpression of OsMKK6 activated the *OsMPK3* and enhanced the cold tolerance of rice [62]. Zhao et al. [59] have reported that the MAP kinase pathway (MEKK1-MKK1/2-MPK4) increased the *CBFs* expression and freezing tolerance by inhibiting the MKK4/5-MPK3/6 cascade. Collectively, the enhanced expression of transcripts for Ca^{2+}, hormones, and ROS in *P. crymophila* activated a complicated signaling cascade, regulating various downstream genes that respond to cold tolerance. These DEGs could be intriguing candidates to investigate during *P. crymophila* seedling cold stress responses.

Role of the circadian clock and photosynthesis in the cold response

Studies have shown that core components of the circadian clock, *CCA1* (*Circadian clock-associated 1*) and *LHY* (*Late-elongating hypocotyl*), play an active role in *CBF* expression, while the nocturnal component, *pseudoresponse regulator* (*PRR*), acts as a repressor of *CBF* expression [16, 63, 64]. A cold-induced clock component *GI* (*GIGANTEA*) can also regulate cold responses in a CBF-independent manner, positively regulates cold stress in Arabidopsis [16, 63, 64]. In *P. crymophila*, *PcPRRs*, *PcLHYs*, and *PcGIs* DEGs were enhanced under cold (Fig. 6F), which indicated the circadian clock that may be an efficient way to increase cold tolerance in *P. crymophila*.

PSII is one of the most sensitive components of photosynthesis [65, 66]. The decline in photosynthesis under cold stress is mainly due to cold stress-induced inhibition of the activity of key enzymes associated with photosynthesis [17, 54]. The LHC (Light-harvesting complex) of photosynthetic antenna proteins (PAP) can rapidly capture light energy to promote photosynthesis in plants [14, 16]. In *P. crymophila*, we found that most of photosynthesis-related DEGs were down-regulated (especially in leaves) (Fig. 6F). These results confirm that *P. crymophila* may adapt to low temperature by reducing leaf photosynthesis and reducing energy loss.

Role of the carbohydrate metabolism under cold stress

Plant sugars serve as energy reserves, free radical scavengers, signaling molecules, and compounds that enhance plant responses to biotic and abiotic stresses. Consequently, carbohydrates are regarded as pivotal factors in plant response and adaptation to cold stress [25, 67]. In this study, DEGs involved in carbohydrate metabolism, including starch synthesis and sugars synthase-related genes, such as UDP-glucose pyrophosphorylase gene (*PcUSP*), beta-glucosidase gene (*PcBGLU28*), galactinol-sucrose galactosyltransferase gene (*PcRFS*) were up-regulated in roots, stems and leaves under cold. Besides, sucrose synthase genes (*PcSUS4*) and beta-glucosidase gene (*PcBGLU32*) were up-regulated both in stems and leaves under cold, beta-fructofuranosidase genes (*PcCIN6*, *PcCIN7*) and ATP-dependent 6-phosphofructokinase gene (*PcPFK3*) were up-regulated in roots under cold (Fig. 6G). These results confirm that *P. crymophila* may have adapted to cold by up-regulating genes in the carbohydrates biosynthetic pathway to increase starch accumulation and sugar accumulation.

Cold tolerance hub genes selected by WGCNA

Weighted Gene Co-expression Network Analysis (WGCNA) serves as a powerful tool for identifying cold tolerance candidate genes through modular gene co-expression networks, enabling systematic investigation of stress tolerance mechanisms in plants [3, 13]. Our application of WGCNA revealed nine cold-responsive hub genes in *P. crymophila*, with *PcABCC2*, *PcABC1K7*, and *PcCTR1*

emerging as potential key regulators in cold signaling pathways (Fig. S7) [68–70]. The *PcABCC2* gene, belonging to the ABCC subfamily of ATP-binding cassette (ABC) transporters, showed functional conservation with its homolog in alfalfa (*Medicago sativa*) where *ABCC3* enhances freezing tolerance through MAPK signaling pathway modulation [68]. Notably, our findings demonstrated significant cold-induced upregulation of *PcABCC2* (Fig. S7), suggesting its potential involvement in MAPK-mediated cold response mechanisms. We observed increased activity of two critical kinase proteins under cold stress: Protein ACTIVITY OF BC1 COMPLEX KINASE 7 (ABC1K7) and Serine/threonine protein kinase CTR1 (CTR1) (Fig. S7). Previous studies indicate that *ABC1K7* homologs (*ABC1K7/8*) mediate crosstalk between ABA and ROS signaling pathways [69], suggesting *PcABC1K7* may coordinate ABA-ROS interactions during cold adaptation. The ETH signaling component CTR1, known to enhance cold tolerance in Arabidopsis [50, 70], showed conserved functionality in *P. crymophila*, implying *PcCTR1*'s potential role in ETH-mediated cold response regulation. This integrated analysis demonstrates WGCNA's effectiveness in elucidating complex cold response networks, revealing three candidate regulators (*PcABCC2*, *PcABC1K7*, and *PcCTR1*) that potentially coordinate MAPK, ABA-ROS, and ETH signaling pathways to enhance cold tolerance in *P. crymophila*. Furthermore, this investigation uncovered significant up-regulation of *PcBLH1* [71] and *PcFTSH1* [72] genes associated with chlorophyll synthesis, and arginine biosynthesis-related gene *PcCARB* [73], indicating their important role in responding to cold stress in *P. crymophila* (Fig. S7). In short, these genes may serve as potential targets for future research aimed at improving plant cold tolerance.

Candidate gene-based EST-SSR molecular marker-assisted selection and application in genetic diversity analysis

EST-SSR (Expressed Sequence Tag-derived Simple Sequence Repeat) molecular markers offer distinct advantages in molecular breeding through their direct association with functional genes, enabling precise marker-assisted selection. Unlike traditional SSRs developed from non-coding regions, EST-SSRs demonstrate enhanced reproducibility, functional relevance, and breeding utility due to their intrinsic linkage to expressed trait-related sequences [21, 74]. Previous applications include Zheng et al. [20]. who effectively clustered *E. sibiricus* germplasms by flowering period using candidate flowering gene-based EST-SSR markers, and Xiao et al. [75]. who developed cold-responsive EST-SSR markers (*ICE1*, *CBF*, *NAC*) for oil palm (*Elaeis guineensis*) with direct breeding applicability. These markers enable genotype-phenotype correlations, significantly advancing cold-tolerance crop breeding. In this study, we developed two novel EST-SSR markers (P37 and P148) derived from cold tolerance candidate genes *PcGA2ox3* and *PcERF013*, respectively. These markers effectively discriminated cold-tolerant *P. crymophila* from three less-resistant *Poa* congeners (Fig. S8), demonstrating their diagnostic potential. Functional characterization of these two genes in *P. crymophila* revealed distinct cold adaptation mechanisms: *PcGA2ox3* likely enhances cold tolerance through GA catabolism, stabilizing DELLA proteins that activate CBF1/3-mediated expression of cold-responsive genes [50]. *PcERF013*, an AP2/ERF transcription factor, regulates osmoprotectant biosynthesis and membrane stabilization genes via direct binding to GCC-box/DRE cis-elements [42]. Both markers showed cold-inducible expression patterns in roots and leaves (Fig. 6A, D), confirming their functional involvement in cold response. While these EST-SSRs effectively identified cold-resistant genotypes, environmental variability partially attenuated interspecific differentiation among the four *Poa* species, emphasizing the importance of integrating multi-trait selection strategies in breeding programs.

In this study, the polymorphic information content (PIC) values of the 29 primer pairs ranged from 0.22 to 0.42, with a mean value of 0.35 (Table S14). This result is similar to a previous related study on *E. nutans*, in which the PIC values of 14 pairs of EST-SSR primers for pendulous lancelet ranged from 0.22 to 0.37, with a mean value of 0.32 [21]. However, the PIC values in this study were low compared to those of barley (PIC values for 49 pairs of EST-SSR primers for barley ranged from 0.08 to 0.75, with a mean value of 0.46) [76]. This result may be due to the fact that the individual plant materials were used for analysis in this study, whereas other studies used population level materials and different study materials may also be one of the reasons. In the present study, it was found that *P. pratensis* var. anceps and *P. pratensis* were closely related genetically (Fig. 9A, D). The results of this study were partially different from the previous genetic diversity study of 31 germplasms of the *Poa* using ISSR [77]. This may be due to the fact that these markers are expressed sequence markers associated with cold tolerance, and their detection sites also fail to represent the entire genome, which is a limitation for genetic diversity evaluation.

Conclusions

In this research, the cold tolerance of four *Poa* species was comprehensively evaluated, and the order of cold tolerance was as follows: *P. crymophila* > *P. botryoides* > *P. pratensis* var. anceps > *P. pratensis*. The key genes and molecular pathways related to cold tolerance were identified, and the response mechanism of cold tolerance in *P. crymophila* was revealed. The Ca^{2+} signaling, ROS signaling, hormone signaling, circadian clock, and photosynthesis related DEGs are coupled to TFs and

play important roles in response to cold stress through triggering a cascade of downstream *CORs*, *CORs* activations further modulates each tissue's cellular metabolic homeostasis and enhanced tolerance (Fig. 10), and most of the DEGs were induced in the early stage of cold stress (3 d). Compared with roots, DEGs in the stems

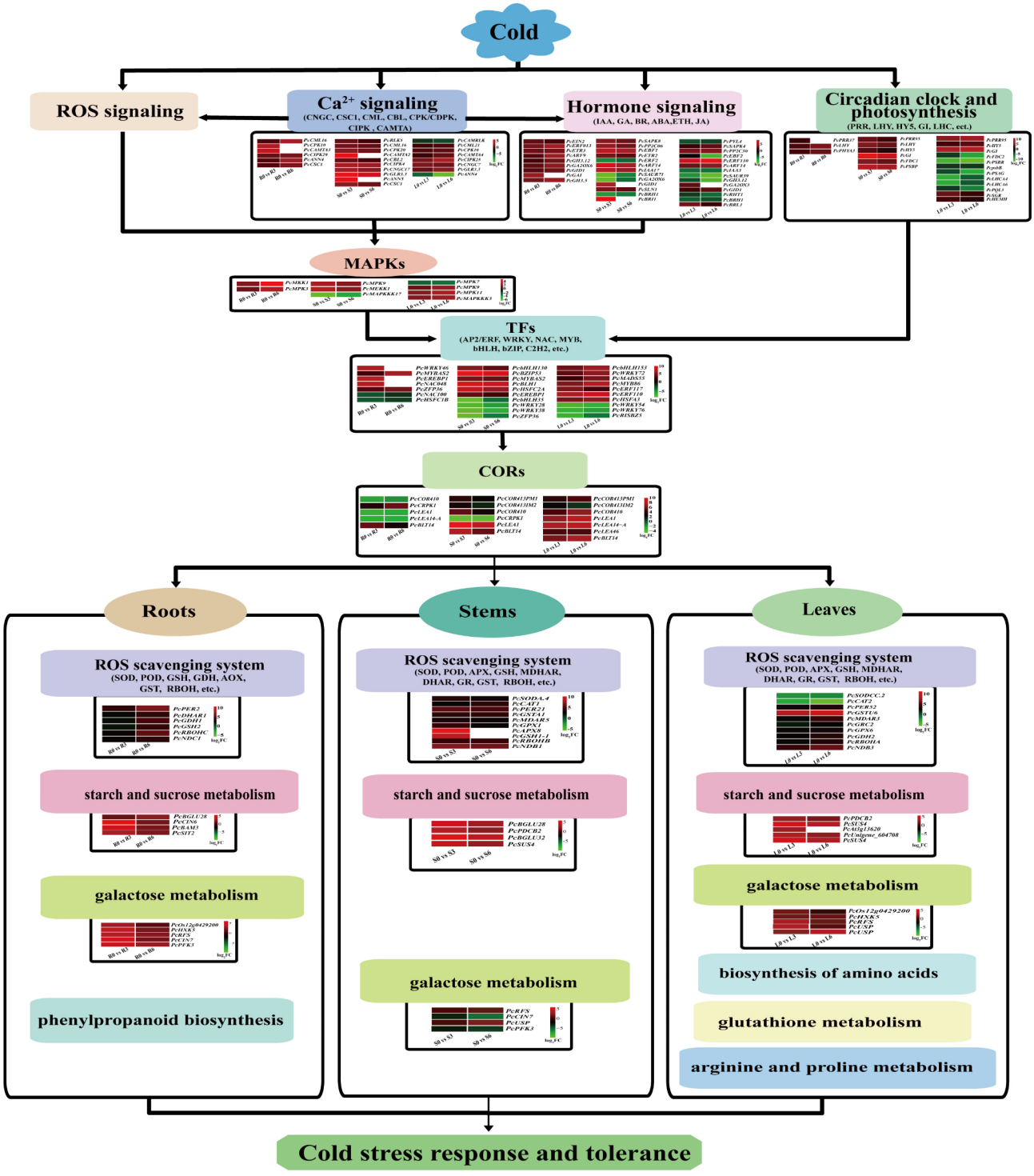

Fig. 10 Schematic diagram of the signaling pathways involved in the cold response mechanism of *P. crymophila*. The model was constructed based on the major cold response components identified in this report and previously described plant abiotic stress pathway schemes. The differential expression analysis between the control/cold conditions in the *P. crymophila* were compared as follows: control root (R0) vs. 4 °C treatment for 3 d (R3), R0 vs. 4 °C treatment for 6 d (R6), control shoot (S0) vs. 4 °C treatment for 3 d (S3), S0 vs. 4 °C treatment for 6 d (S6), control leaf (L0) vs. 4 °C treatment for 3 d (L3), L0 vs. 4 °C treatment for 6 d (L6). Heat maps showing the red and green indicate up-regulated and down-regulated expression pattern of the gene, respectively

and leaves of *P. crymophila* were more active under cold stress. In addition, WGCNA identified nine hub genes that may be involved in *P. crymophil*a responses to cold stress. 29 candidate gene-based EST-SSRs were used to conduct molecular genetic diversity analysis and cold tolerance screening of different cold-resistant *Poa* species. UPGMA cluster and STRUCTURE analysis showed that the 40 *Poa* individuals were clustered into three major groups, with *Poa* species with similar cold tolerance being grouped together. The markers P37 (*PcGA2ox3*) and P148 (*PcERF013*) could distinguish *P. crymophila* from the other three *Poa* species. Altogether, our results provide important insights into the future understanding of the biochemical and molecular mechanisms underlying the response of *P. crymophila* to cold stress, and also lays a foundation for molecular marker-assisted selection for cold tolerance improvement of *Poa* species. Furthermore, the functional genes involved have the potential to be used in the development of new forage grass varieties for enhanced productivity and stress tolerance.

Supplementary Information

The online version contains supplementary material available at https://doi.org/10.1186/s12870-025-06383-3.

Supplementary Material 1

Supplementary Material 2

Acknowledgements
Not applicable.

Author contributions
LB. T.: Investigation, Data curation, Writing-original draft, Software. YY. Z: Software, Writing-review & editing, Discussions. HH. L.: Software, Discussions. YS. Q.: Software, Discussions. HZ. W.: Methodology, HQ. L.: Methodology. WG. X.: Investigation, Conceptualization, Funding acquisition, Writing-review & editing.

Funding
This research was funded by the Leading Scientist Project of Qinghai Province (2023-NK-147), Leading Scientist Project of Gansu Province (23ZDKA013), CARS (CARS-34) and Gansu Provincial Science and Technology Major Projects (22ZD6NA007).

Data availability
The data sets supporting the results of this article are available in the NCBI's Sequence Read Archive (SRA) database (accession number: SRP470158 (https://www.ncbi.nlm.nih.gov/Traces/study/?acc= SRP470158&go=go).

Declarations

Ethics approval and consent to participate
All methods were performed in accordance with the relevant guidelines and regulations.

Consent for publication
Not applicable.

Competing interests
The authors declare no competing interests.

Author details
[1]State Key Laboratory of Herbage Improvement and Grassland Agro-Ecosystems, Key Laboratory of Grassland Livestock Industry Innovation, Ministry of Agriculture and Rural Affairs, College of Pastoral Agriculture Science and Technology, Lanzhou University, Lanzhou 730020, China

Received: 18 June 2024 / Accepted: 11 March 2025
Published online: 19 March 2025

References

1. Wang LT, Jian ZL, Wang PC, Zhao LL, Chen KK. Combined physiological responses and differential expression of drought-responsive genes preliminarily explain the drought resistance mechanism of *Lotus corniculatus*. Funct Plant Biol. 2023;50(1):46–57.
2. Ding YL, Yang SH. Surviving and thriving: how plants perceive and respond to temperature stress. Dev Cell. 2022;57(8):947–58.
3. Dong R, Luo B, Tang L, Wang QX, Lu ZJ, Chen C, Yang F, Wang S, He J. A comparative transcriptomic analysis reveals a coordinated mechanism activated in response to cold acclimation in common Vetch (*Vicia sativa* L). BMC Genomics. 2022;23(1):814.
4. Yan T, Sun M, Su R, Wang XZ, Lu XD, Xiao YH, Deng HB, Liu X, Tang WB, Zhang GL. Transcriptomic profiling of cold stress-induced differentially expressed genes in seedling stage of *Indica* rice. Plants. 2023;12(14):2675.
5. Gusain S, Joshi S, Joshi R. Sensing, signalling, and regulatory mechanism of cold-stress tolerance in plants. Plant Physiol Biochem. 2023;197:107646.
6. Nouri MZ, Komatsu S. Subcellular protein overexpression to develop abiotic stress tolerant plants. Front Plant Sci. 2013;4:2.
7. Cheng MJ, Cui KS, Zheng MM, Yang T, Zheng JJ, Li XF, Luo X, Zhou Y, Zhang RZ, Yan DH, Yao M, Iqbal MZ, Zhou Q, He R. Physiological attributes and transcriptomics analyses reveal the mechanism response of *Helictotrichon virescens* to low temperature stress. BMC Genomics. 2022;23(1):280.
8. Zhang H, Zhu J, Gong Z, Zhu JK. Abiotic stress responses in plants. Nat Rev Genet. 2022;23(2):104–19.
9. Fursova OV, Pogorelko GV, Tarasov VA. Identification of *ICE2*, a gene involved in cold acclimation which determines freezing tolerance in *Arabidopsis Thaliana*. Gene. 2009;429(1–2):98–103.
10. Shu YJ, Li W, Zhao JY, Zhang SJ, Xu HY, Liu Y, Guo CH. Transcriptome sequencing analysis of alfalfa reveals *CBF* genes potentially playing important roles in response to freezing stress. Genet Mol Biol. 2017;40(4):824–33.
11. Zhuo CL, Liang L, Zhao YQ, Guo ZF, Lu SY. A cold responsive ethylene responsive factor from *Medicago falcata* confers cold tolerance by up-regulation of polyamine turnover, antioxidant protection, and proline accumulation. Plant Cell Environ. 2018;41(9):2021–32.
12. Ritonga FN, Chen S. Physiological and molecular mechanism involved in cold stress tolerance in plants. Plants. 2020;9(5):560.
13. Zhou Q, Cui Y, Dong SW, Luo D, Fang LF, Shi ZJ, Liu WX, Wang ZY, Nan ZB, Liu ZP. Integrative physiological, transcriptome, and metabolome analyses reveal the associated genes and metabolites involved in cold stress response in common Vetch (*Vicia sativa* L). Food Energy Secur. 2023;12(4):0–0.
14. Zhu JK. Abiotic stress signaling and responses in plants. Cell. 2016;167(2):313–24.
15. Zhang H, Jiang CJ, Ren JY, Dong JL, Shi XL, Zhao XH, Wang XG, Wang J, Zhong C, Zhao SL. An advanced lipid metabolism system revealed by transcriptomic and lipidomic analyses plays a central role in peanut cold tolerance. Front Plant Sci. 2020;11:1110.
16. Qi LJ, Shi YT, Terzaghi W, Yang SH, Li JG. Integration of light and temperature signaling pathways in plants. J Integr Plant Biol. 2022;64(2):393–411.
17. Cheng MJ, Pan ZY, Cui KS, Zheng JJ, Luo X, Chen YJ, Yang T, Wang H, Li XF, Zhou Y, Lei X, Li Y, Zhang R, Iqbal MZ, He R. RNA sequencing and weighted gene co-expression network analysis uncover the hub genes controlling cold tolerance in *Helictotrichon virescens* seedlings. Front Plant Sci. 2022;13:938859.
18. Min XY, Liu ZP, Wang YR, Liu WX. Comparative transcriptomic analysis provides insights into the coordinated mechanisms of leaves and roots response to cold stress in common Vetch. Ind Crops Prod. 2020;158(0):112949–112949.
19. Li L, Han CL, Yang JW, Tian ZQ, Jiang RY, Yang F, Jiao KM, Qi ML, Liu LL, Zhang BZ. Comprehensive transcriptome analysis of responses during cold stress in wheat (*Triticum aestivum* L). Genes. 2023;14(4):844.
20. Zheng YY, Zhang ZY, Wan YY, Tian JY, Xie WG. Development of EST-SSR markers linked to flowering candidate genes in *Elymus sibiricus* L. based on RNA sequencing. Plants. 2020;9(10):1371.

21. Zhao YQ, Zhang JC, Zhang ZY, Xie WG. *Elymus nutans* genes for seed shattering and candidate gene-derived EST-SSR markers for germplasm evaluation. BMC Plant Biol. 2019;19(1):102.
22. Zou FL, Hu QW, Li HD, Lin J, Liu YC, Sun FL. Dynamic disturbance analysis of grasslands using neural networks and Spatiotemporal indices fusion on the Qinghai-Tibet plateau. Front Plant Sci. 2022;12:760551.
23. Li XY, Wang Y, Hou XY, Chen Y, Li CX, Ma XR. Flexible response and rapid recovery strategies of the plateau forage *Poa crymophila* to cold and drought. Front Plant Sci. 2022;13:970496.
24. Hua QY, Yu Y, Dong SK, Li S, Shen H, Han YH, Zhang J, Xiao JN, Liu SL, Dong QM. Leaf spectral responses of *Poa crymophila* to nitrogen deposition and climate change on Qinghai-Tibetan plateau. Agric Ecosyst Environ. 2019;284(0):106598–106598.
25. Fu JJ, Miao YJ, Shao LH, Hu TM, Yang PZ. De Novo transcriptome sequencing and gene expression profiling of *Elymus nutans* under cold stress. BMC Genomics. 2016;17(1):870.
26. Dong W, Ma X, Jiang H, Zhao C, Ma H. Physiological and transcriptome analysis of *Poa pratensis* Var. Anceps Cv. Qinghai in response to cold stress. BMC Plant Biol. 2020;20(1):362.
27. Wang X, Yu C, Liu Y, Yang L, Li Y, Yao W, Cai Y, Yan X, Li S, Cai Y. *GmFAD3A*, a ω-3 fatty acid desaturase gene, enhances cold tolerance and seed germination rate under low temperature in rice. Int J Mol Sci. 2019;20(15):3796.
28. Bai WP, Li HJ, Hepworth SR, Liu HS, Liu LB, Wang GN, Ma Q, Bao AK, Wang SM. Physiological and transcriptomic analyses provide insight into thermotolerance in desert plant zygophyllum Xanthoxylum. BMC Plant Biol. 2023;23(1):7.
29. Xie Y, Lou HJ, Hu YX, Sun XY, Lou YH, Fu JM. Classification of genetic variation for cadmium tolerance in Bermudagrass [*Cynodon dactylon* (L.) Pers.] using physiological traits and molecular markers. Ecotoxicology. 2014;23(6):1030–43.
30. Zheng YY, Wang N, Zhang ZY, Liu WH, Xie WG. Identification of flowering regulatory networks and hub genes expressed in the leaves of *Elymus sibiricus* L. using comparative transcriptome analysis. Front Plant Sci. 2022;13:877908.
31. Jones P, Binns D, Chang HY, Fraser M, Li WZ, McAnulla C, McWilliam H, Maslen J, Mitchell A, Nuka G. InterProScan 5: genome-scale protein function classification. Bioinformatics. 2014;30(9):1236–40.
32. Eddy SR. Profile hidden Markov models. Bioinformatics. 1998;14(9):755–63.
33. Anders S, Huber W. 2010. Differential expression analysis for sequence count data. Genome Biol. 2010;11(10):R106.
34. Adnan M, Morton G, Hadi S. Analysis of *RpoS* and *BolA* gene expression under various stress-induced environments in planktonic and biofilm phase using $^{2-\Delta\Delta CT}$ method. Mol Cell Biochem. 2011;357(1–2):275–82.
35. Wang Y, Li XY, Li CX, He Y, Hou XY, Ma XR. The regulation of adaptation to cold and drought stresses in *Poa crymophila* Keng revealed by integrative transcriptomics and metabolomics analysis. Front Plant Sci. 2021;12:631117.
36. Xing JY, Tan JJ, Feng HQ, Zhou ZJ, Deng M, Luo HB, Deng ZP. Integrative proteome and phosphoproteome profiling of early cold response in maize seedlings. Int J Mol Sci. 2022;23(12):6493.
37. Kakar N, Jumaa SH, Redoña ED, Warburton ML, Reddy KR. Evaluating rice for salinity using pot-culture provides a systematic tolerance assessment at the seedling stage. Rice. 2019;12(1):57.
38. Huseynova IM, Rustamova SM, Suleymanov SY, Aliyeva DR, Mammadov AC, Aliyev JA. Drought-induced changes in photosynthetic apparatus and antioxidant components of wheat (*Triticum durum* Desf.) varieties. Photosynth Res. 2016;130(1–3):215–23.
39. Sun FL, Chen Q, Chen QJ, Jiang MH, Gao WW, Qu YY. Screening of key drought tolerance indices for cotton at the flowering and boll setting stage using the dimension reduction method. Front Plant Sci. 2021;12:619926.
40. Qi WL, Wang F, Ma L, Qi Z, Liu SQ, Chen C, Wu JY, Wang P, Yang CR, Wu Y, Sun WC. Physiological and biochemical mechanisms and cytology of cold tolerance in *Brassica Napus*. Front Plant Sci. 2020;11:1241.
41. Tian Y, Peng KK, Lou GC, Ren ZP, Sun XZ, Wang ZW, Xing JP, Song CH, Cang J. Transcriptome analysis of the winter wheat *Dn1* in response to cold stress. BMC Plant Biol. 2022;22(1):277.
42. Cai XX, Chen Y, Wang Y, Shen Y, Yang JK, Jia BW, Sun XL, Sun MZ. A comprehensive investigation of the regulatory roles of *OsERF096*, an *AP2/ERF* transcription factor, in rice cold stress response. Plant Cell Rep. 2023;42(12):2011–22.
43. Liu CT, Ou SJ, Mao BG, Tang JY, Wang W, Wang HR, Cao SY, Schläppi MR, Zhao BR, Xiao GY. Early selection of *bZIP73* facilitated adaptation of Japonica rice to cold climates. Nat Commun. 2018;9(1):3302.
44. Wang DZ, Jin YN, Ding XH, Wang WJ, Zhai SS, Bai LP, Guo ZF. Gene regulation and signal transduction in the ICE-CBF-COR signaling pathway during cold stress in plants. Biochemistry. 2017;82(10):1103–17.
45. Novillo F, Medina J, Salinas J. Arabidopsis *CBF1* and *CBF3* have a different function than *CBF2* in cold acclimation and define different gene classes in the CBF Regulon. Proc Natl Acad Sci U S A. 2007;104(52):21002–7.
46. Adhikari L, Baral R, Paudel D, Min D, Makaju SO, Poudel HP, Acharya JP, Missaoui AM. Cold stress in plants: strategies to improve cold tolerance in forage species. Plant Stress. 2022;4(0):100081–100081.
47. Shah FA, Ni J, Yao YY, Hu H, Wei RY, Wu LF. Overexpression of Karrikins receptor gene *Sapium Sebiferum KAI2* promotes the cold stress tolerance via regulating the redox homeostasis in *Arabidopsis Thaliana*. Front Plant Sci. 2021;12:657960.
48. Eremina M, Rozhon W, Poppenberger B. Hormonal control of cold stress responses in plants. Cell Mol Life Sci. 2016;73(4):797–810.
49. Lv XZ, Li HZ, Chen XX, Xiang X, Guo ZX, Yu JQ, Zhou YH. The role of calcium-dependent protein kinase in hydrogen peroxide, nitric oxide and ABA-dependent cold acclimation. J Exp Bot. 2018;69(16):4127–39.
50. Waadt RS, Seller CA, Hsu PK, Takahashi Y, Munemasa S, Schroeder JI. Plant hormone regulation of abiotic stress responses. Nat Rev Mol Cell Biol. 2022;23(10):680–94.
51. Du H, Wu N, Fu J, Wang SP, Li XH, Xiao JH, Xiong LZ. A GH3 family member, *OsGH3-2*, modulates auxin and abscisic acid levels and differentially affects drought and cold tolerance in rice. J Exp Bot. 2012;63(18):6467–80.
52. Shi Q, Zhang YY, To VT, Shi J, Zhang DB, Cai WG. Genome-wide characterization and expression analyses of the aux-in/indole-3-acetic acid (Aux/IAA) gene family in barley (*Hordeum vulgare* L). Sci Rep. 2020;10(1):10242.
53. Kagale S, Divi UK, Krochko JE, Keller WA, Krishna P. Brassinosteroid confers tolerance in *Arabidopsis Thaliana* and *Brassica Napus* to a range of abiotic stresses. Planta. 2007;225(2):353–64.
54. Deng SX, Ma J, Zhang LL, Chen FJ, Sang ZY, Jia ZK, Ma LY. De Novo transcriptome sequencing and gene expression profiling of *Magnolia wufengensis* in response to cold stress. BMC Plant Biol. 2019;19(1):321.
55. Xiang N, Hu JG, Yan SJ, Guo XB. Plant hormones and volatiles response to temperature stress in sweet corn (*Zea Mays* L.) seedlings. J Agric Food Chem. 2021;69(24):6779–90.
56. Mishra N, Jiang CK, Chen L, Paul A, Chatterjee A, Shen GX. Achieving abiotic stress tolerance in plants through antioxidative defense mechanisms. Front Plant Sci. 2023;14:1110622.
57. Mittler R, Zandalinas SI, Fichman Y, Van Breusegem F. Reactive oxygen species signalling in plant stress responses. Nat Rev Mol Cell Biol. 2022;23(10):663–79.
58. Kantakhoo J, Imahori Y. Antioxidative responses to pre-storage hot water treatment of red sweet pepper (*Capsicum annuum* L.) fruit during cold storage. Foods. 2021;10(12):3031.
59. Zhao CZ, Wang PC, Si T, Hsu CC, Wang L, Zayed O, Yu ZP, Zhu YF, Dong J, Tao WA. MAP kinase cascades regulate the cold response by modulating *ICE1* protein stability. Dev Cell. 2017;43(5):618–e6295.
60. Guo H, Wu TK, Li SX, He Q, Yang ZL, Zhang WH, Gan Y, Sun PY, Xiang GL, Zhang HY, Deng H. The methylation patterns and transcriptional responses to chilling stress at the seedling stage in rice. Int J Mol Sci. 2019;20(20):5089.
61. Cheng GM, Zhang LY, Wang HT, Lu JH, Wei HL, Yu SY. Transcriptomic profiling of young cotyledons response to chilling stress in two contrasting cotton (*Gossypium hirsutum* L.) genotypes at the seedling stage. Int J Mol Sci. 2020;21(14):5095.
62. Xie GS, Kato H, Imai R. Biochemical identification of the OsMKK6-OsMPK3 signalling pathway for chilling stress tolerance in rice. Biochem J. 2012;443(1):95–102.
63. Hung FY, Chen FF, Li CL, Chen C, Chen JH, Cui YH, Wu KQ. The LDL1/2-HDA6 histone modification complex interacts with *TOC1* and regulates the core circadian clock components in Arabidopsis. Front Plant Sci. 2019;10:233.
64. Li YP, Shi YT, Li M, Fu DY, Wu SF, Li JG, Gong ZZ, Liu HT, Yang SH. The CRY2–COP1–HY5–BBX7/8 module regulates blue light-dependent cold acclimation in Arabidopsis. Plant Cell. 2021;33(11):3555–73.
65. Wu H, Wu ZX, Wang YH, Ding J, Zheng YL, Tang H, Yang L. Transcriptome and metabolome analysis revealed the freezing resistance mechanism in 60-year-old overwintering *Camellia sinensis*. Biology (Basel). 2021;10(10):996.
66. Ren C, Fan PG, Li SH, Liang ZC. Advances in Understanding cold tolerance in grapevine. Plant Physiol. 2023;192(3):1733–46.
67. Cui P, Li YX, Cui CK, Huo YR, Lu GQ, Yan HQ. Proteomic and metabolic profile analysis of low-temperature storage responses in *Ipomoea Batata* lam. Tuberous roots. BMC Plant Biol. 2020;20(1):435.

68. Wang X, Kang WJ, Wu F, Miao JM, Shi SL. Comparative transcriptome analysis reveals new insight of alfalfa (*Medicago sativa* L.) cultivars in response to abrupt freezing stress. Front Plant Sci. 2022;13:798118.
69. Manara A, DalCorso G, Furini A. The role of the atypical kinases *ABC1K7* and *ABC1K8* in abscisic acid responses. Front Plant Sci. 2016;7:366.
70. Huang JY, Zhao XB, Bürger M, Chory J, Wang XC. The role of ethylene in plant temperature stress response. Trends Plant Sci. 2023;28(7):808–24.
71. Meng LH, Fan ZQ, Zhang QW, Gao Y, Deng YK, Zhu BZ, Zhu HL, Chen JY, Shan W, Yin XR. *BEL1-LIKE HOMEODOMAIN 11* regulates Chloroplast development and chlorophyll synthesis in tomato fruit. Plant J. 2018;94(6):1126–40.
72. Wu QF, Han TT, Yang L, Wang Q, Zhao YX, Jiang D, Ruan X. The essential roles of *OsFtsH2* in developing the Chloroplast of rice. BMC Plant Biol. 2021;21(1):445.
73. Ke NJ, Kumka JE, Fang MX, Weaver B, Burstyn JN, Bauer CE. *RedB*, a member of the CRP/FNR family, functions as a transcriptional redox brake. Microbiol Spectr. 2022;10(5):e0235322.
74. Zhang ZY, Xie WG, Zhao YQ, Zhang JC, Wang N, Ntakirutimana F, Yan JJ, Wang YR. EST-SSR marker development based on RNA-sequencing of *E. sibiricus* and its application for phylogenetic relationships analysis of seventeen *Elymus* species. BMC Plant Biol. 2019;19(1):235.
75. Xiao Y, Zhou L, Xia W, Mason AS, Yang Y, Ma Z, Peng M. Exploiting transcriptome data for the development and characterization of gene-based SSR markers related to cold tolerance in oil palm (*Elaeis guineensis*). BMC Plant Biol. 2014;14:384.
76. Zhang MA, Mao WH, Zhang GP, Wu F. Development and characterization of polymorphic EST-SSR and genomic SSR markers for Tibetan annual wild barley. PLoS ONE. 2014;9(4):e94881.
77. Zhao GQ, Liu H, Liu M. ISSR-based genetic diversity analysis of *Poa* L. Acta Agrestia Sinica. 2011;19(05):781–6. (In Chinese).

Publisher's note